

**Project Report  
NASA/L-1**

# **Cockpit Weather Information (CWI) Program Summary Report for FY1993**

**M.P. Matthews  
S.D. Campbell  
T.J. Dasey**

**3 June 1994**

---

**Lincoln Laboratory**

**MASSACHUSETTS INSTITUTE OF TECHNOLOGY**

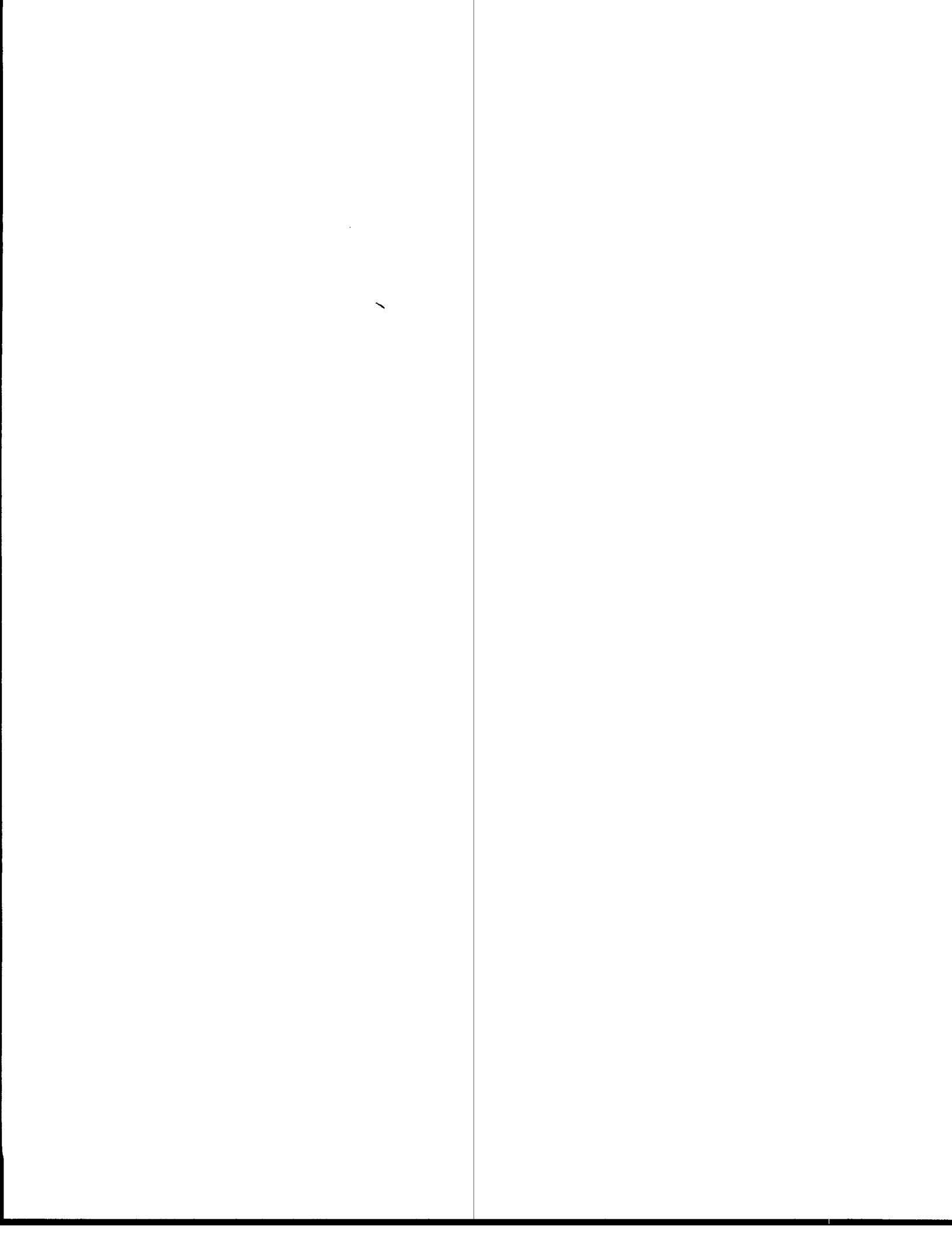
*LEXINGTON, MASSACHUSETTS*



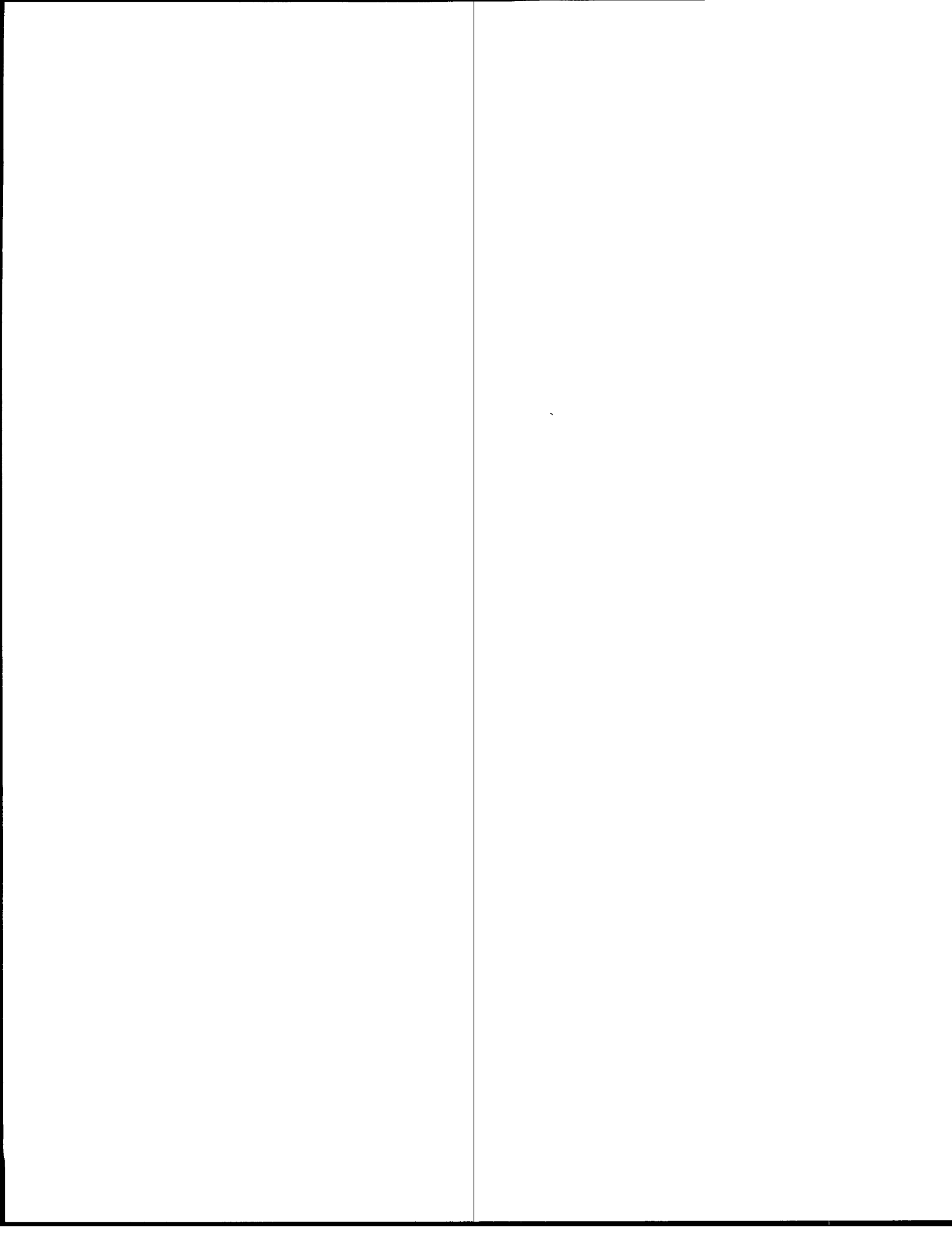
Prepared for NASA Langley.

Document is available to the public through  
the National Technical Information Service,  
Springfield, Virginia 22161.

**ACCESSION NUMBER**  
364619  
JUL 1 1994  
ARCHIVES  
MIT LINCOLN LABORATORY



**This document is disseminated under the sponsorship of NASA Langley Research Center in the interest of information exchange. The United States Government assumes no liability for its contents or use thereof.**



## ABSTRACT

The Cockpit Weather Information (CWI) program is funded through NASA Langley Research Center by the joint NASA/FAA Integrated Airborne Wind Shear program. Its objective is to integrate ground-based and airborne wind shear information into crew-centered hazard warning information. Two research aircraft (University of North Dakota (UND) Cessna Citation and the NASA ATOPS B737) and three avionics manufacturers (Bendix, Westinghouse, and Rockwell Collins) participated in microburst penetration flights to provide data to compute the aircraft hazard index, or F factor, and compare the results with F factors computed by three methods that used the TDWR radar data from each of the microburst penetrations. The flights and flight support were conducted at the Lincoln Laboratory Terminal Doppler Weather Radar (TDWR) testbed located 10 kilometers to the south of Orlando International Airport.

The first method of computing F factor from TDWR radar data used the TDWR microburst detection algorithm, the second involved processing the TDWR base data, and the third used the advanced microburst detection techniques being developed in the Integrated Terminal Weather System (ITWS). The TDWR microburst algorithm performed well in detecting the microbursts penetrated but provided little information to compute an accurate F factor. Investigation into the methods used to alert the crew of microbursts from airborne wind shear detection systems lead to the development of a shear map from the TDWR base data. Results showed an excellent correlation between the F factor from the shear map and the aircraft. The third method involved identifying microbursts using the shear map developed in the second method and computing an F factor from these microburst shapes. This new detection strategy, known as the Lincoln Advanced Microburst Detection Algorithm (LAMBDA), provides a much more accurate F factor computation from a ground-based system.

The key goals of the CWI program have been accomplished. During the four-year program, over 120 microburst penetrations were conducted and the data were processed for comparison. The data link and cockpit display were successfully demonstrated in real time with the UND Cessna Citation and the NASA ATOPS B737 in the Orlando penetration flights. F factor comparisons for the aircraft and TDWR data have resulted in significant improvements in the wind shear detection and reporting techniques.



## ACKNOWLEDGMENTS

The authors wish to acknowledge the contributions of their colleagues to the work reported here. William Rooney and Robert DeMillo wrote the cockpit server software. Peter Daley programmed the Argus cockpit display. Anthony Berke was instrumental in writing the data reduction and analysis software. Paul Morin, Mike O'Donnell and Charlie LeBell performed much of the data reduction and generated many of the plots shown in this report.

The authors also wish to thank personnel at the Lincoln-operated TDWR testbed radar in Orlando, FL for their efforts. Paul Biron, Mark Isaminger, Nat Fischer, and Doug Piercey provided real-time support for the test flights. Stan Dajnak was instrumental in establishing the modem link to the NASA hangar and resolving interface problems.

Thanks are also due to the University of North Dakota personnel who operated the Cessna Citation II aircraft. Roger Tilbury and Fred Remer were instrumental in planning and carrying out the flight program. Rodger Copp was responsible for the cockpit display installation and Martin Brown provided valuable information on reducing the aircraft data. Leon Osborne and Ron Rinehart provided administrative support for the flight program.

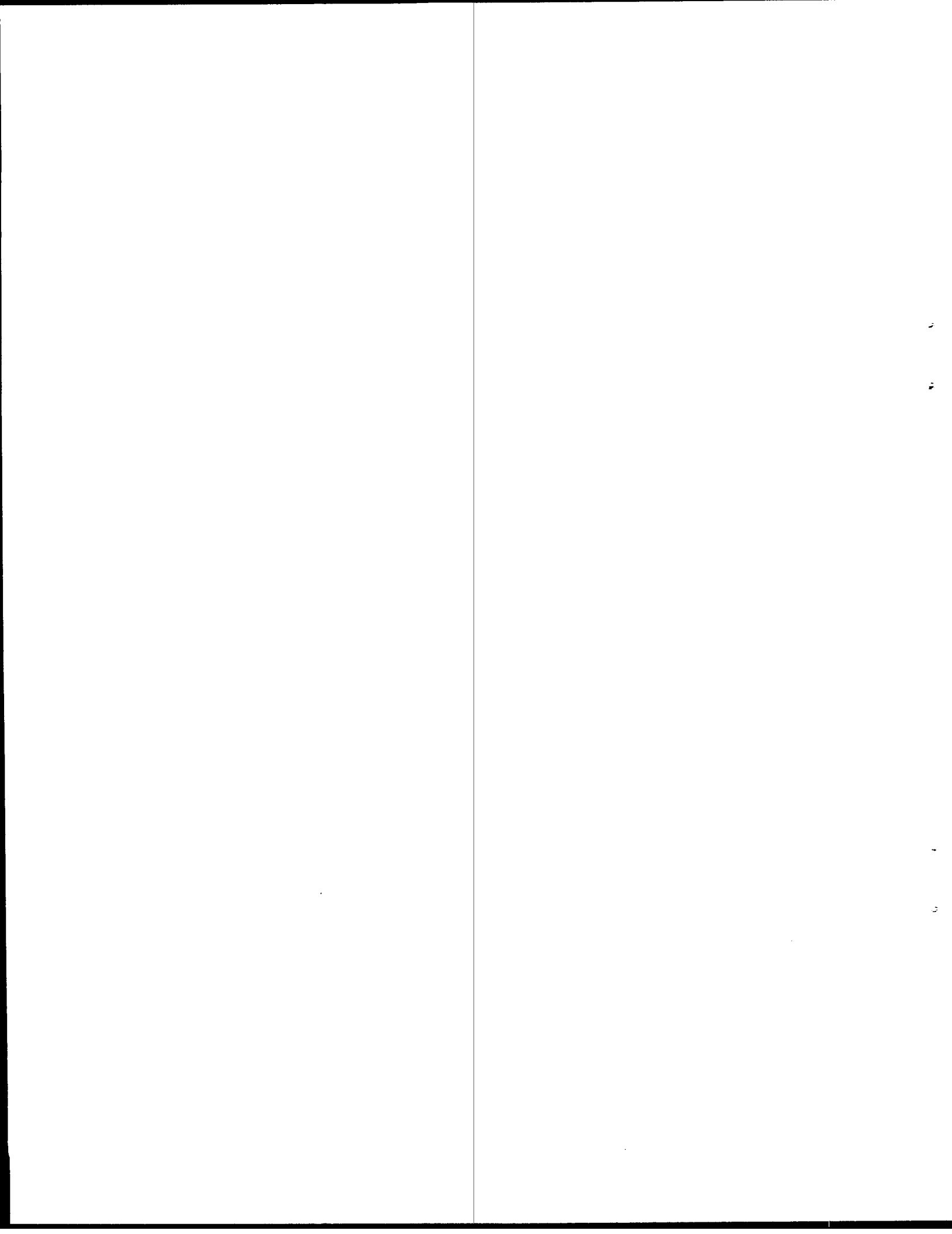
Also, the authors wish to extend their thanks to the avionics manufacturers who provided the data reduction support for their respective aircraft. Mike Eide and Bruce Mathews of Westinghouse and Roy Robertson of Rockwell Collins International were all helpful in assimilating the aircraft data to the TDWR data.

Finally, the authors wish to thank Roland Bowles and David Hinton of NASA Langley Research Center for their efforts in initiating this program at Lincoln and providing technical assistance throughout the project.



## TABLE OF CONTENTS

<u>Section</u>	<u>Page</u>
Abstract	iii
Acknowledgments	v
List of Illustrations	ix
List of Tables	x
1. INTRODUCTION	1
2. TERMINAL DOPPLER WEATHER RADAR	3
3. FLIGHT OPERATIONS AND SUMMARY	7
3.1 University of North Dakota Cessna Citation II	7
3.2 NASA Langley Research Center ATOPS B737	12
3.3 Avionics Manufacturers	17
4. DATALINK AND COCKPIT DISPLAY	25
4.1 University of North Dakota Cessna Citation II	25
4.2 NASA Langley Research Center ATOPS B737	26
5. DATA PROCESSING	31
5.1 University of North Dakota Cessna Citation II	32
5.2 NASA Langley Research Center ATOPS B737	33
5.3 Avionics Manufacturers	33
5.4 Terminal Doppler Weather Radar	33
5.4.1 TDWR Microburst Algorithm	34
5.4.2 TDWR Shear Map	36
5.5 Integrated Terminal Weather System	38
6. F FACTOR ESTIMATION	39
6.1 F Factor Estimates from TDWR Microburst Algorithm	39
6.2 F Factor Estimates from TDWR Shear Map	39
6.3 F Factor Estimates using Altitude Correction	40
6.4 Estimating Horizontal Term of F Factor	43
6.5 Estimating Vertical Term of F Factor	45
6.6 F Factor Estimates from ITWS Microburst Algorithm	46
7. IMPROVED RUNWAY ALERTING STRATEGY	55
8. SUMMARY	57
GLOSSARY	59
REFERENCES	61



## LIST OF ILLUSTRATIONS

<u>Figure</u>		<u>Page</u>
1.	Illustration of a microburst impacting runway 18 approach.	5
2.	University of North Dakota Center for Aerospace Studies Cessna Citation II.	9
3.	NASA B737 ATOPS aircraft.	13
4.	Westinghouse BAC-111 aircraft.	19
5.	Rockwell Collins Saberliner aircraft.	23
6.	University of North Dakota data link system.	25
7.	University of North Dakota cockpit display.	27
8.	NASA ATOPS data link system.	29
9.	Data processing overview.	31
10.	Illustration of a microburst shape from shear segments.	34
11.	Illustration of microburst continuity.	36
12.	Least-squares-fit shear computation.	37
13.	TDWR alarm vs. aircraft total F factor.	39
14.	TDWR shear map vs. aircraft total F factor.	40
15.	Comparison of aircraft altitude during microburst penetration and TDWR radar beam altitude.	41
16.	Altitude profile used in Oseguera & Bowles model.	41
17.	TDWR shear map vs. aircraft total F factor using altitude profile correction.	42
18.	TDWR shape vs. aircraft horizontal F factor at F total peak time.	43
19.	TDWR shear map vs. aircraft horizontal F factor at F total peak time.	44
20.	TDWR shear map vs. aircraft horizontal F factor at F total peak time using altitude profile correction.	44
21.	TDWR alarm vs. aircraft vertical F factor at F total peak time.	45
22.	Downdraft profile across radius of microburst event in Vicroy Model.	46
23.	TDWR shear map vs. aircraft vertical F factor at F total peak time.	47
24.	ITWS shape vs. aircraft horizontal F factor at F total peak time.	48
25.	ITWS shape vs. aircraft vertical F factor at F total peak time.	49

## LIST OF ILLUSTRATIONS (CONTINUED)

<u>Figure</u>	<u>Page</u>
26. F factor estimated from TDWR and ITWS for NASA case on 6/15/91 in Orlando.	49
27. Shear map for NASA case on 6/15/91 in Orlando overlaid with TDWR shapes.	51
28. Shear map for NASA case on 6/15/91 in Orlando overlaid with ITWS shapes.	53

## LIST OF TABLES

<u>Table</u>	<u>Page</u>
1. UND Microburst Penetrations	11
2. NASA Microburst Penetrations	15
3. Westinghouse Microburst Penetrations	17
4. Rockwell Microburst Penetrations	21

## 1. INTRODUCTION

This project report summarizes the Cockpit Weather Information (CWI) program at M.I.T. Lincoln Laboratory. The CWI program is funded through NASA Langley Research Center by the joint NASA/FAA Integrated Airborne Wind Shear program. The Fiscal Year 1993 concludes the fourth year of a projected four-year program.

The overall purpose of the CWI program is to integrate ground-based and airborne wind shear information to provide crew-centered hazard warning. One aspect of the Lincoln effort was to provide support for the microburst penetration flights conducted in Orlando, FL. Test flights were conducted by two research aircraft and three avionics manufacturers, with the support of the Lincoln operated Terminal Doppler Weather Radar (TDWR) testbed located 10 kilometers to the south of Orlando International Airport (MCO). Under the NASA program, Lincoln processed the aircraft data and the TDWR data for each of the microburst penetrations and compared a hazard index, called the F factor (Bowles, 1990). Post-flight processing was performed on four of the five test aircraft and analysis was performed to compare the aircraft data with three methods of equating the F factor from the TDWR radar.

The first F factor estimation method involved using the TDWR microburst detection algorithm, the second involved processing the TDWR base data, and the third involved using the advanced microburst detection techniques being developed in the Integrated Terminal Weather System (ITWS). Results have shown that the TDWR microburst algorithm performed well in detecting the microbursts penetrated but provided little information to compute an accurate F factor. Investigation into the methods used to alert the crew of microbursts from airborne wind shear detection systems lead to the development of a shear map from the TDWR base data. Results showed an excellent correlation between the F factor from the shear map and the aircraft. The final method involved identifying microbursts using the shear map developed in the second method and computing an F factor from these microburst shapes. Results, have shown that this new detection strategy, known as the Lincoln Advanced Microburst Detection Algorithm (LAMBDA), provides a much more accurate F factor computation from a ground-based system.

An interagency agreement was developed between NASA and the Air Force which described a number of tasks to be accomplished by Lincoln Laboratory. The Lincoln tasks will be discussed in the following sections of the report. Section 2 describes the TDWR program conducted by the FAA and the radar characteristics of the testbed TDWR. Section 3 describes the flight operations and summarizes the flights conducted by the two research aircraft and the three avionics manufacturers over a four-year period. Section 4 describes a real-time data link and cockpit display system developed for this project. Section 5 describes the post-flight data processing and the microburst algorithms developed under TDWR and ITWS. Section 6 compares the F factor estimation techniques with the *in situ* aircraft data. Section 7 introduces a proposed new wind shear runway alerting strategy. The conclusions of the four-year program are summarized in Section 8.

The key goals of the CWI program have been accomplished. During the four-year program, over 120 microburst penetrations were conducted and processed for comparison. The data link and cockpit display were successfully demonstrated in real-time with the University of North Dakota Cessna Citation and the NASA Advanced Transport Operating System (ATOPS) B737 in the Orlando penetrations. Finally, F factor comparisons for the aircraft and TDWR data were

carried out and results have lead to significant improvements in the wind shear detection and reporting techniques.

An additional task was accomplished under the supervision of Dr. John Hansman of the M.I.T. Aeronautics and Astronautics Department. This task involved evaluation of a crew-centered alerting procedure. The results of this task were presented in previous reports (Wanke and Hansman, 1990;1992).

## 2. TERMINAL DOPPLER WEATHER RADAR

The Federal Aviation Administration (FAA) initiated the Terminal Doppler Weather Radar (TDWR) program in the mid-1980s to detect low level wind shear in the airport terminal area. Low level wind shear was determined to be the cause of several major aircraft accidents between 1964 and 1985. The TDWR system, to be installed at 45 major airports in the United States, is intended to warn pilots of wind shear and help them avoid this hazard on approach and departure.

Since 1983 Lincoln Laboratory has been involved with developing, testing, and evaluating the Doppler radar technology to perform timely detection and reporting of hazardous wind shear. During the summer of 1985 Lincoln deployed the Doppler radar to Memphis, TN to begin collecting data for development of the automated detection algorithms. Since 1985 the radar has been moved to Huntsville, AL in 1986, Denver, CO in 1987 and 1988, Kansas City, MO in 1989, and finally to Orlando, FL in 1990. This report deals with data collected in the subtropical environment of Orlando, FL during the summers of 1990, 1991, and 1992 only.

The principal requirements for the initial TDWR are timely, reliable microburst detection, including probability of detection greater than 90 percent, with a false-alarm probability of less than 10 percent. The system must provide this information automatically to Air Traffic Control with no need for meteorological interpretation. TDWR also must be capable of detecting gust fronts and providing the ATC with a 20-minute warning of gust front arrival at the airport. Finally, the system provides information about the location of precipitation within 50 nautical miles of the airport.

The Lincoln operated testbed TDWR (designated FL-2) uses an antenna 28 feet in diameter and a powerful signal processing system to collect the radar data (Bernella, 1991). Since the summer of 1990, the testbed TDWR has been operating as a C-band radar with 1.1 ms 250 kw pulses at Doppler mode, pulse repetition frequency (PRF) from 1066-1930 Hz. This pencil beam antenna operates with a 0.5 degree beamwidth with sidelobes less than -27dB. When weather is in the airport area a plan position indicator (PPI) volume scan is performed over the airport sector every 2.5 minutes, with a surface tilt every one minute. If there is no significant weather present near the airport, the radar operates in a monitor mode, taking full 360° volume scans every five minutes.

The radar base data are subjected to a number of data processing algorithms to provide the best possible edited data to the microburst algorithms. First, clutter suppression is done with high pass filters then point-target editing and ground clutter residue removal are performed. This is done to ensure that the clutter near the ground does not affect the algorithms. Next, range obscuration editing is performed using low PRF scan data. This ensures that out of trip weather does not contaminate the algorithm performance. Finally, velocity unfolding is performed using information from dual scans at different PRFs and spatial discontinuities in the velocity field (Sykes and Stevens, 1991).

The next step in the TDWR system is to process the edited base data through the automated detection algorithms. The algorithms use extensive site adaptable parameters to facilitate performance optimization in a variety of environments. The microburst detection algorithm fits race tracked shaped icons around groups of radar radial velocity segments that show sufficient loss along their length. Each icon is assigned a peak-to-peak velocity difference within the icon. This

loss value is based upon the number of segments within the shape and ranges from the segment with the highest loss value to the 85th percentile shear within the shape based upon the number of segments. Other algorithms present in the TDWR system are designed to detect rotation within a cell, convergence at mid-levels of the atmosphere, divergence aloft, and reflectivity features aloft ranging from a dry cell (region of 15dBZ reflectivity and greater) to reflectivity cores (regions greater than 45dBZ). The TDWR microburst algorithm uses these features to verify the presence of features aloft that are usually present within a microburst-producing storm cell. Other aspects of the TDWR system are gust front detection and prediction, and storm motion tracking.

The next function of the TDWR system is to distribute this information in a timely manner to the Air Traffic Control personnel. This is done with two types of displays: a geographical situation display (GSD) and an alphanumeric "ribbon" display terminal (RDT). The RDT reports runway specific impacts of wind shear to the local controller. During times of weather impact at the airport, the local controller will use the RDT to verbally communicate the wind shear impact to the pilot. The GSD is situated near the ATC supervisor and depicts the entire weather scenario of the terminal area. The GSD is useful as a supervisor's planning tool, for if a gust front is predicted to impact the airport in 15 minutes, the supervisor can plan runway configuration accordingly.

The TDWR system generates the RDT alerts using a process known as shear integration. The shear integration algorithm ingests both the TDWR microburst algorithm detections and the TDWR gust front algorithm detections. The primary purpose of shear integration is to account for the proximity of the wind shear hazard to the runway approach and departure corridors. For example, if a microburst is detected by the TDWR algorithms and the center is located one mile to the west of the runways, some portion of the microburst will be in the runway corridor. However, the entire strength of the microburst would not be experienced when flying through the runway corridor. Figure 1 illustrates an example of a 50 knot microburst that is located on the approach to runway 18. Notice how only a small portion of the shape resides in the flight path. One possible method for generating the RDT message is to issue a microburst alert with a 50 knot loss. However, this would not be representative of the loss an aircraft would experience. Therefore, shear integration attempts to estimate the loss an aircraft would experience flying along the approach path.

Shear integration begins by assuming that a microburst is a region of uniform shear. For example, a 50 knot microburst over two miles is a region of shear with uniform 25 knots/mile of shear. Then for each runway corridor, the algorithm defines 1/4 kilometer long regions. Each region is then assigned a shear value. Finally, the algorithm totals the shear for all the regions along the runway. This total is then multiplied by the distance over which it was computed to give a loss value for the runway corridor. This loss value is the change in headwind to tailwind across the runway corridor. The algorithm also keeps track of the location of first encounter and this information is all presented on the RDT as follows:

18A MBA 30k- 3MF 120 08

In the above example, the controller would read the alert to the pilot as, "18 Arrival Microburst Alert thirty knot loss three miles final." The first characters represent the runway and whether the alert is for approach or departure. The second group of characters specify whether there is a wind

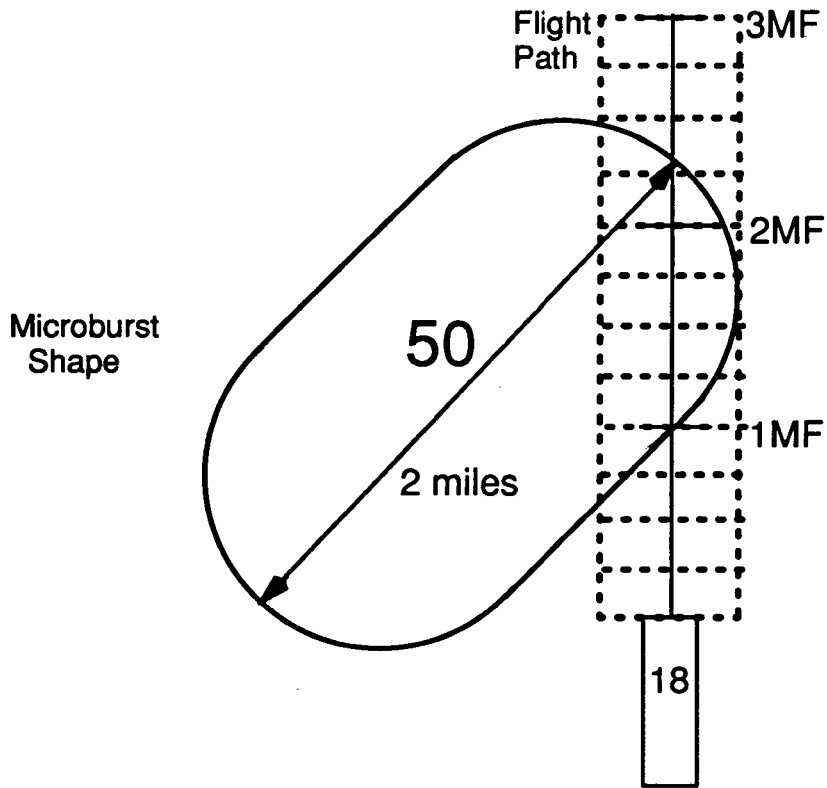
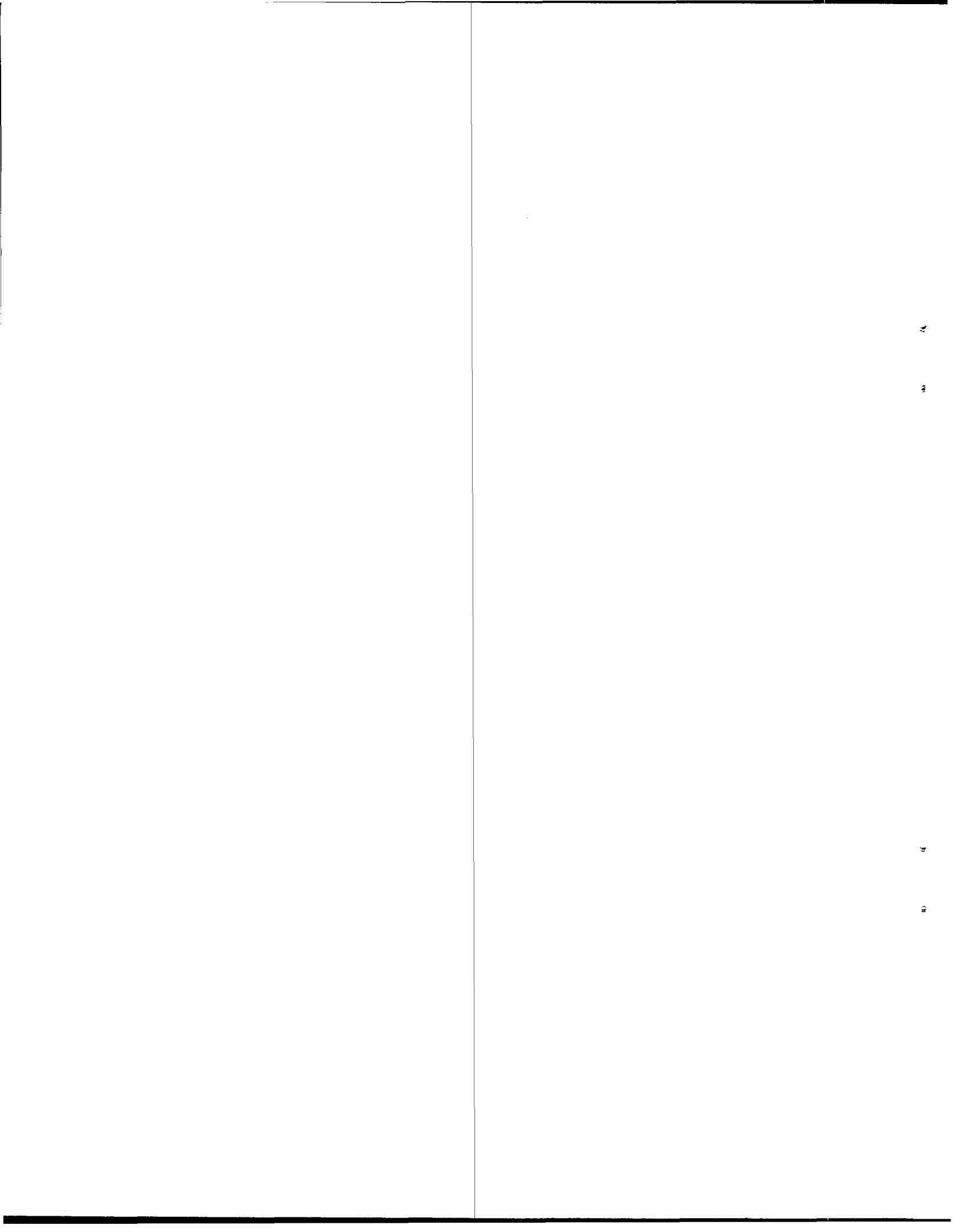


Figure 1. Illustration of a microburst impacting runway 18 approach.

shear alert or a microburst alert. The third group indicates the strength in knots and whether the wind shear is a loss or a gain. The final group of characters specifies the location of first encounter. The ribbon displays limits the location of first encounter on approach to three miles and on departure to two miles.



### 3. FLIGHT OPERATIONS AND SUMMARY

During the summers of 1990, 1991, and 1992, five different research aircraft flew instrumented microburst penetrations in Orlando, Florida. These microburst penetrations were conducted under the surveillance of the Lincoln operated testbed TDWR. Prior to each aircraft's operations, various meetings were held to discuss flight safety considerations as well as what each participant expected from the others. This section will describe the operational procedures for each aircraft and give a summary of the data recorded during the aircraft operations.

The testbed TDWR system in Orlando, FL provided both oral and graphical data link to the pilots of the research aircraft. In many instances this was as simple as reporting verbally to a research pilot the peak reflectivity and loss within a microburst. In some instances, a member of the personnel at the TDWR testbed was using the base data of the TDWR system to data link a waypoint to the aircraft for display on the moving map display. At the most sophisticated level, this involved data linking the microburst icons to the aircraft and displaying the icons on a moving map display.

#### 3.1. UNIVERSITY OF NORTH DAKOTA CESSNA CITATION II

The University of North Dakota Center for Aerospace Studies operated their Cessna Citation II shown in Figure 2 during the summer of 1990. The Citation aircraft was operated for eight weeks (6/16/90 to 7/25/90 and 9/17/90 to 9/28/90), for a total of 25 flights. A total of 80 recorded events were accomplished under TDWR coverage. These events included a well documented penetration of a 50-kt microburst over the airport on July 7, 1992.

Before operations began in Orlando, a meeting was held with Lincoln, NASA and UND personnel to discuss flight safety considerations. To minimize the hazard of these activities, the Citation aircraft was to be flown through microbursts at a nominal speed of 160 kts (~80m/s). Penetrations were to be flown with a clean configuration (landing gear up and flaps up) and were always planned as missed approaches. All aircraft activity was to be coordinated with the Lincoln testbed personnel and Air Traffic Control.

The Citation instrument data was recorded in flight on nine-track tape at a 24 Hz rate. These data were converted by UND in post processing to a 1 Hz rate data by averaging and/or sampling. Plots of this data were produced by UND and transcripts of cockpit voice conversations were supplied to Lincoln. The aircraft also included a forward-looking infrared radiometer system for airborne wind shear detection, manufactured by Turbulence Prediction Systems (TPS). TPS also recorded the Citation instrumentation data on 5.25-inch floppy disks by tapping a serial line driving an Amiga computer. These floppy disks were made available to NASA and Lincoln for translation to internal record formats.

Unlike the other research aircraft involved in this study, the UND aircraft made rapid maneuvers during flight and flew at a variety of altitudes. Altitude ranged from 27 meters while on takeoff to well over 700 meters while in flight. Since microburst outflows usually do not extend above 450 meters above ground level (AGL), all events above 500 meters were removed from this data analysis. Also removed from this study were any events where the aircraft performed a sharp bank during the microburst encounter. These cases were unacceptable for analysis because many of the comparison techniques use the ground speed and true air speed of the aircraft in the



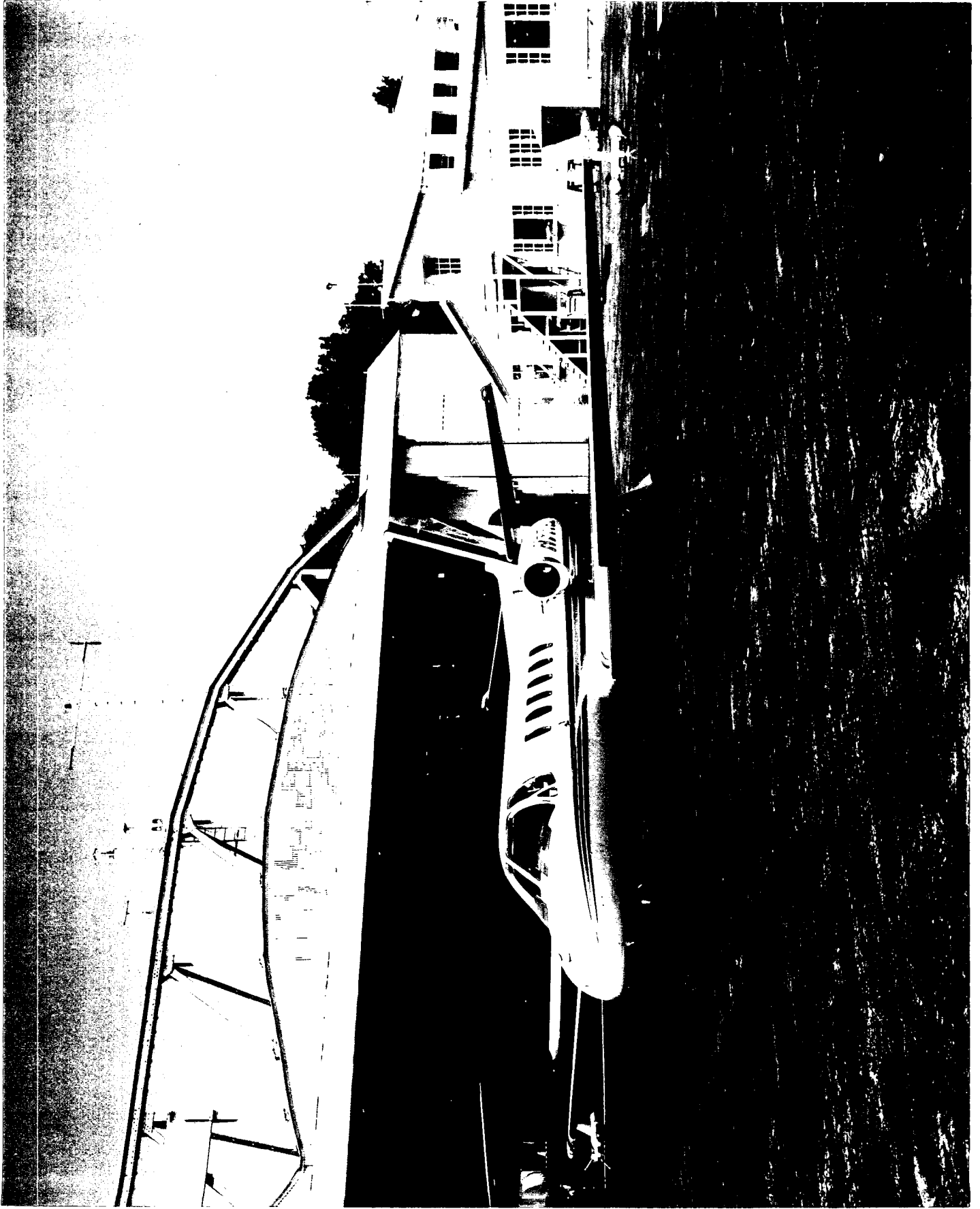


Figure 2. University of North Dakota Center for Aerospace Studies Cessna Citation II.



analysis equations. Also removed from the list were events where the aircraft did not penetrate a microburst icon and also did not experience any shear. However, all events where the aircraft did encounter a microburst but did not encounter a microburst icon were included. Table 1 lists all of the UND microburst events meeting the requirements to be accepted as quality cases, a total of 41. The peak F factor is the maximum F factor reported by the aircraft after appropriate filtering by the data processing algorithms.

**Table 1.**  
**UND Microburst Penetrations**

DATE	EVENT TIME (UT)	LOCATION OF EVENT (RANGE/AZIMUTH)	PEAK AIRCRAFT In Situ F factor	AIRCRAFT EVENT NUMBER
6/21/90	21:19:40	19.0 / 357	0.106	UND01
6/22/90	19:57:51	13.8 / 350	0.121	UND02
	19:59:31	11.4 / 002	0.041	UND03
	20:08:46	14.3 / 000	0.029	UND04
6/24/90	19:24:47	5.5 / 005	0.025	UND05
	19:39:34	3.7 / 060	0.074	UND06
	19:45:50	7.0 / 061	0.060	UND07
7/04/90	20:27:33	3.5 / 057	0.076	UND24
	20:49:36	16.5 / 023	0.061	UND26
	20:52:16	18.4 / 035	0.132	UND27
	20:53:46	25.7 / 045	0.113	UND28
	20:57:50	24.7 / 040	0.072	UND29
	20:58:42	21.4 / 034	0.036	UND30
7/07/90	18:55:58	14.0 / 012	0.152	UND37
	19:03:29	14.0 / 011	0.072	UND38
	19:09:19	15.6 / 009	0.063	UND39
7/08/90	18:33:51	6.9 / 001	0.050	UND40
	19:55:41	7.7 / 018	0.049	UND45
	20:05:50	16.1 / 358	0.053	UND46
	20:07:19	8.1 / 357	0.056	UND47
	20:08:15	2.3 / 345	0.042	UND48
	20:21:24	4.7 / 332	0.050	UND49
	20:31:47	15.1 / 357	0.078	UND50
7/09/90	17:29:42	11.3 / 013	0.138	UND53
7/11/90	18:40:41	2.3 / 007	0.096	UND54

**Table 1. (Continued)  
UND Microburst Penetrations**

DATE	EVENT TIME (UT)	LOCATION OF EVENT (RANGE/ AZIMUTH)	PEAK AIRCRAFT In Situ F factor	AIRCRAFT EVENT NUMBER
9/17/90	20:48:17	11.3 / 317	0.112	UND61
	20:51:48	11.8 / 318	0.072	UND63
	20:56:04	8.2 / 304	0.090	UND64
	20:58:48	7.7 / 299	0.104	UND65
	21:02:28	10.0 / 322	0.076	UND66
9/17/90	21:03:23	7.0 / 302	0.063	UND67
	21:06:24	6.8 / 296	0.026	UND68
	21:07:34	10.4 / 326	0.073	UND69
	21:11:18	8.6 / 328	0.054	UND70
	21:15:12	8.0 / 321	0.063	UND71
9/28/90	20:30:03	7.6 / 358	0.072	UND84
	20:39:44	5.1 / 357	0.063	UND85
	20:48:17	11.4 / 000	0.039	UND87
	21:02:17	19.4 / 277	0.102	UND90
	21:06:07	19.9 / 279	0.051	UND91

### 3.2. NASA LANGLEY RESEARCH CENTER ATOPS B737

The NASA B737, shown in Figure 3, operated in Orlando during the summers of 1991 and 1992 for a total of four weeks (6/9/91 to 6/21/91 and 8/11/92 to 8/25/92), with eleven days of wind shear activity. A total of 51 microbursts penetrations were accomplished during this period, with the strongest event occurring on June 20, 1991. Table 2 lists all of the NASA microburst events meeting the requirements to be accepted as quality cases, a total of 51.

Due to its larger size, the NASA B737 aircraft required a minimum speed of 210 knots in the clean configuration and flew at nominal speeds of 220–240 knots. The NASA aircraft limited the flight altitude to a minimum of 750 ft. and would not fly through regions of greater than 55dBZ reflectivity. One benefit of the NASA approach was that during each microburst penetration, the flight crew would line up on level flight approximately five miles prior to the encounter. Also, because the Doppler radar is only capable of measuring the wind component along a radial, flight paths were generally flown along a TDWR radial.



Figure 3. NASA B737 ATOPS aircraft.



**Table 2.  
NASA Microburst Penetrations**

<b>DATE</b>	<b>EVENT TIME (UT)</b>	<b>LOCATION OF EVENT (RANGE/ AZIMUTH)</b>	<b>PEAK AIRCRAFT In Situ F factor</b>	<b>AIRCRAFT EVENT NUMBER</b>
6/15/91	19:29:36	17.8 / 010	0.059	NASA79
	19:38:40	18.4 / 014	0.022	NASA80
	19:52:36	28.6 / 026	0.115	NASA81
	20:30:57	31.8 / 033	0.043	NASA86
6/17/91	18:32:05	16.0 / 351	0.077	NASA95
	18:51:10	28.0 / 015	0.042	NASA97
6/18/91	19:10:20	28.0 / 049	0.027	NASA106
	20:23:45	29.2 / 054	0.089	NASA114
	20:26:36	30.7 / 056	0.048	NASA115
	20:48:26	12.7 / 013	0.091	NASA117
	20:52:59	13.6 / 011	0.049	NASA118
6/19/91	17:27:39	15.4 / 019	0.064	NASA126
	20:31:26	29.3 / 062	0.095	NASA133
	20:52:27	29.4 / 058	0.068	NASA134
6/20/91	20:41:45	28.3 / 021	0.096	NASA142
	20:46:05	28.2 / 020	0.158	NASA143
	20:52:14	27.7 / 022	0.076	NASA144
	20:57:44	27.2 / 021	0.056	NASA145
	21:21:31	7.5 / 030	0.055	NASA148
8/11/92	21:07:04	14.2,-0.5	0.106	NASA483
	21:16:55	17.3,1.9	0.091	NASA484
	21:23:35	14.9,1.5	0.059	NASA485
8/12/92	17:20:15	4.0,16.5	0.093	NASA490
	17:55:53	-5.7,4.8	0.062	NASA493
	20:31:39	15.8,11.6	0.075	NASA501
	20:39:20	22.9,4.5	0.073	NASA502
8/13/92	18:44:19	19.8,1.3	0.060	NASA507a
	18:45:05	25.4,3.4	0.087	NASA507b
	18:49:54	19.7,5.5	0.109	NASA508

**Table 2. (Continued)  
NASA Microburst Penetrations**

DATE	EVENT TIME (UT)	LOCATION OF EVENT (RANGE/AZIMUTH)	PEAK AIRCRAFT In Situ F factor	AIRCRAFT EVENT NUMBER
	18:54:24	20.3,6.1	0.089	NASA509
	18:59:59	21.5,9.7	0.083	NASA510
	19:20:33	22.0,19.0	0.091	NASA512a
	19:23:42	23.1,22.1	0.071	NASA512b
	19:28:29	21.7,25.0	0.048	NASA514
	20:08:22	21.2,-11.4	0.106	NASA518
	20:15:44	22.2,-8.0	0.092	NASA519
	20:29:49	24.4,-1.7	0.066	NASA520
8/14/92	20:28:39	23.8,20.4	0.076	NASA530
8/17/92	22:00:08	20.9,-16.7	0.070	NASA547
	22:03:36	18.7,-17.3	0.145	NASA548
	22:07:54	20.3,-17.0	0.087	NASA549
	22:20:53	26.6,-17.7	0.107	NASA551
	22:29:05	29.1,-16.1	0.147	NASA553
	22:34:03	23.1,-18.2	0.127	NASA554
	22:38:14	22.1,-20.2	0.132	NASA555
	22:43:06	25.6,-17.2	0.093	NASA556
	22:50:19	21.9,-21.8	0.068	NASA558
	22:54:16	23.0,-24.0	0.069	NASA559
	23:01:29	29.8,-1.6	0.061	NASA560
8/19/92	21:23:09	3.0,8.6	0.049	NASA571
	21:33:25	18.3,13.0	0.120	NASA573
	21:37:09	19.4,12.4	0.073	NASA574

The NASA B737 was equipped with several types of wind shear detection sensors. The first system was the second generation accelerometer-based reactive wind shear detection system developed at NASA Langley. This system was used to compute *in situ* wind shear measurements for truthing the forward-looking wind shear systems. The second system was a passive-infrared forward-looking radiometer developed by TPS. The third system was an airborne 10.6 micron Doppler laser. It was built by Lockheed Missiles and Space under contract to NASA Langley. The final system was an airborne Doppler weather radar developed at NASA Langley.

During operations of the NASA ATOPS aircraft, two-way radio communication was used to relay valuable weather information from the TDWR testbed to the aircraft. During the summer of 1991 this was performed by one of the radar operators at the tested TDWR. The radar operator informed the aircraft crew of the location and severity of the microbursts in the region being scanned by the TDWR radar. The most important function of the radar operator was to provide the aircraft crew with all of the information necessary to plan the short term (10–15 minute) and long term (1–2 hours) objectives. During the summer of 1992 an expert meteorologist from NASA Langley was present at the radar to perform these functions. Also, during operations the experimental data link display described in Section 4.2 was used to maneuver the aircraft for microburst penetrations and for flight safety decisions before penetration (Lewis, 1992; Hinton, 1993).

Data from the ATOPS aircraft was recorded in flight on magnetic tapes and converted in post flight processing to 3.5-inch floppy disk format. Video recordings were made from cameras placed in the nose of the aircraft, mounted on the tail of the aircraft, and cameras trained on various displays and personnel located within the aircraft.

### 3.3. AVIONICS MANUFACTURERS

Three avionics manufacturers tested their airborne Doppler weather radar systems in Orlando during the summers of 1991 and 1992: Westinghouse, Rockwell–Collins, and Bendix. The manufacturers followed various flight safety requirements, similar to those used by UND. For most of the aircraft penetration, *in situ* data were available from the manufacturers for comparison with the radar data.

The Westinghouse BAC–111, shown in Figure 4, flew during the summers of 1991 and 1992. Data was unavailable from the summer of 1991 due to the limited equipment on the Westinghouse aircraft, and the microbursts penetrated by the aircraft were outside of the TDWR scan sector. During the summer of 1992, the aircraft was in Orlando just after a lightning strike at the TDWR testbed. Therefore, radar data was unavailable for all but one day of operations. The data for the one day of simultaneous operations included five microburst penetrations with the strongest having an F factor of 0.137. Table 3 lists all of the Westinghouse microburst events meeting the requirements to be accepted as quality cases, a total of five.

**Table 3.**  
**Westinghouse Microburst Penetrations**

DATE	EVENT TIME (UT)	LOCATION OF EVENT (RANGE/ AZIMUTH)	PEAK AIRCRAFT In Situ F factor	AIRCRAFT EVENT NUMBER
7/17/92	19:45:53	20.7,–17.6	0.062	WH1
	19:50:28	18.7,–18.5	0.054	WH2
	20:36:08	11.5,–25.3	0.137	WH6
	20:43:39	10.3,–24.3	0.059	WH7
	20:48:24	7.5,–27.2	0.059	WH8



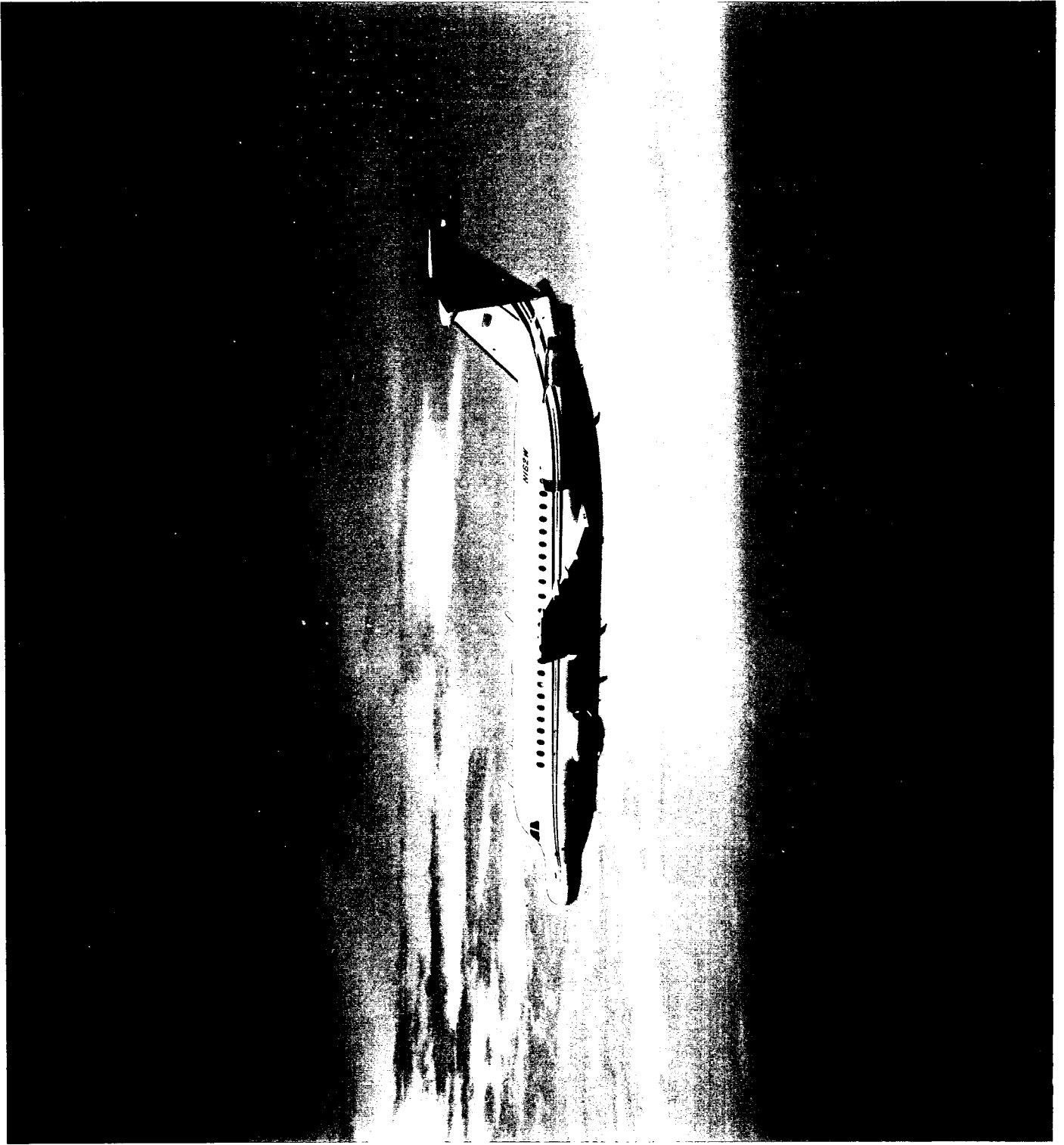


*Figure 4. Westinghouse BAC-II aircraft.*

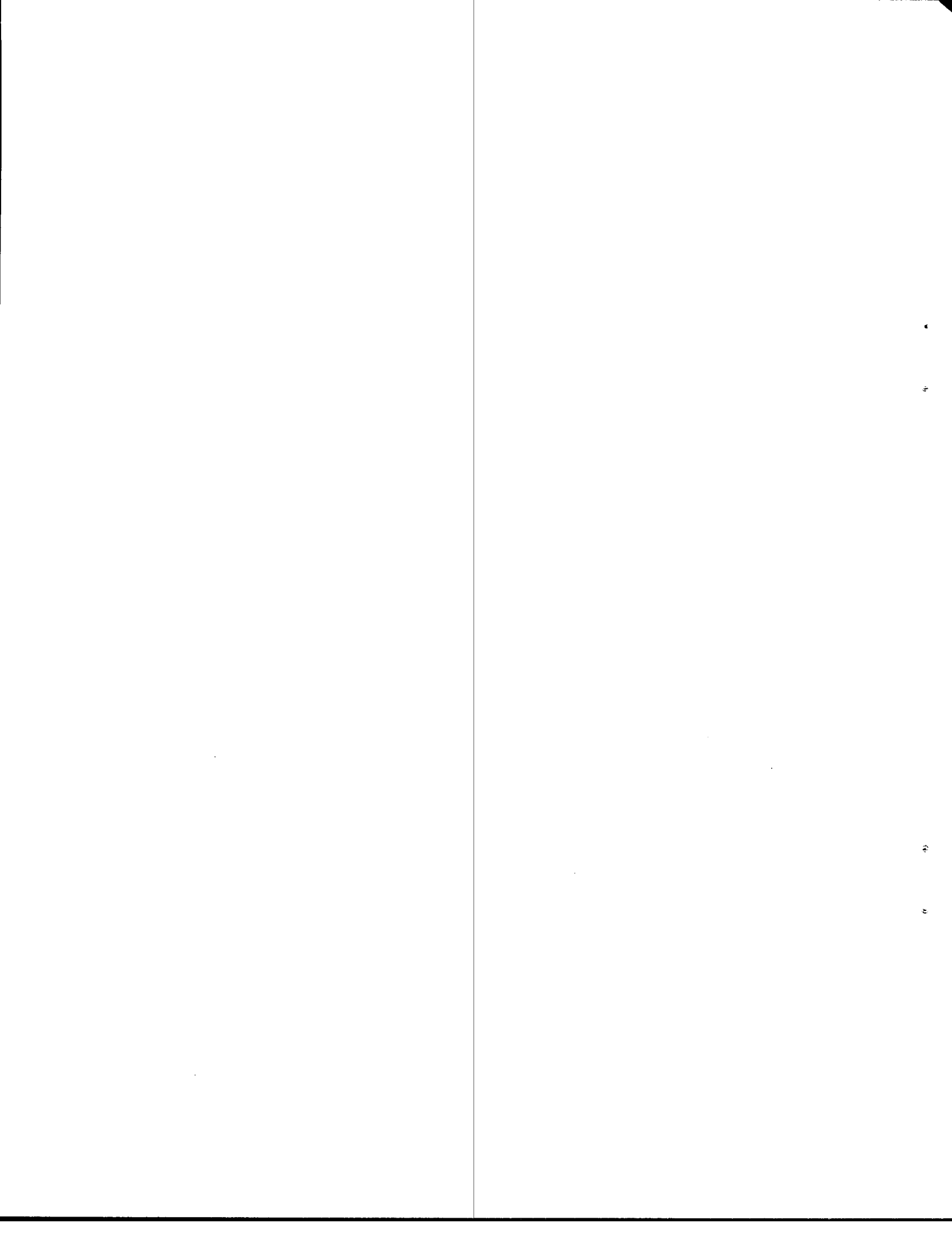


The Rockwell Collins Saberliner shown in Figure 5 flew during the summers of 1991 and 1992. A total of 21 microburst penetrations were conducted under TDWR coverage on six different days (8/22/91 to 8/25/91 and 9/10/92 to 9/11/92). The Rockwell Collins aircraft was able to provide the most comprehensive data from all of the manufacturers' aircraft due to its *in situ* wind shear equipment during both summers. Table 4 lists all of the Rockwell Collins microburst events meeting the requirements to be accepted as quality cases, a total of 20.

Bendix Corporation flew during the summers of 1991 and 1992. Limited data were available from the Bendix aircraft due to the *in situ* equipment on board. Because of the limited usefulness of the Bendix data, it was not included in the microburst penetration database.

**Table 4.**  
**Rockwell Collins Microburst Penetrations**

DATE	EVENT TIME (UT)	LOCATION OF EVENT (RANGE/AZIMUTH)	PEAK AIRCRAFT In Situ F factor	AIRCRAFT EVENT NUMBER
8/22/91	22:09:15	-11.9,-15.5	0.067	RC_91_2.2
	22:11:51	-13.2,-14.3	0.099	RC_91_2.3
	22:27:54	-7.3,-16.5	0.107	RC_91_3.3
8/23/91	21:14:32	-9.7,3.2	0.146	RC_91_5
	21:20:26	-11.9,2.8	0.085	RC_91_6
8/24/91	19:08:06	0.5,6.4	0.088	RC_91_9
8/25/91	20:55:32	-0.3,-17.6	0.032	RC_91_10.1
	20:59:08	5.0,-16.9	0.099	RC_91_10.2
	21:13:39	-2.7,-8.7	0.075	RC_91_11
9/10/92	20:28:30	12.7,-6.1	0.074	RC_92_1
	20:33:12	17.1,-4.2	0.080	RC_92_2
	20:43:13	7.4,15.2	0.072	RC_92_3
9/11/92	21:19:53	15.9,-2.6	0.061	RC_92_7
	21:20:35	11.7,-2.7	0.078	RC_92_8
	21:23:59	12.5,0.0	0.078	RC_92_9
	21:29:24	12.2,0.0	0.063	RC_92_10
	21:39:49	10.5,1.1	0.039	RC_92_14
	21:47:22	13.0,1.4	0.080	RC_92_16
	21:55:09	11.5,3.9	0.079	RC_92_17
	22:03:02	12.6,0.6	0.075	RC_92_18



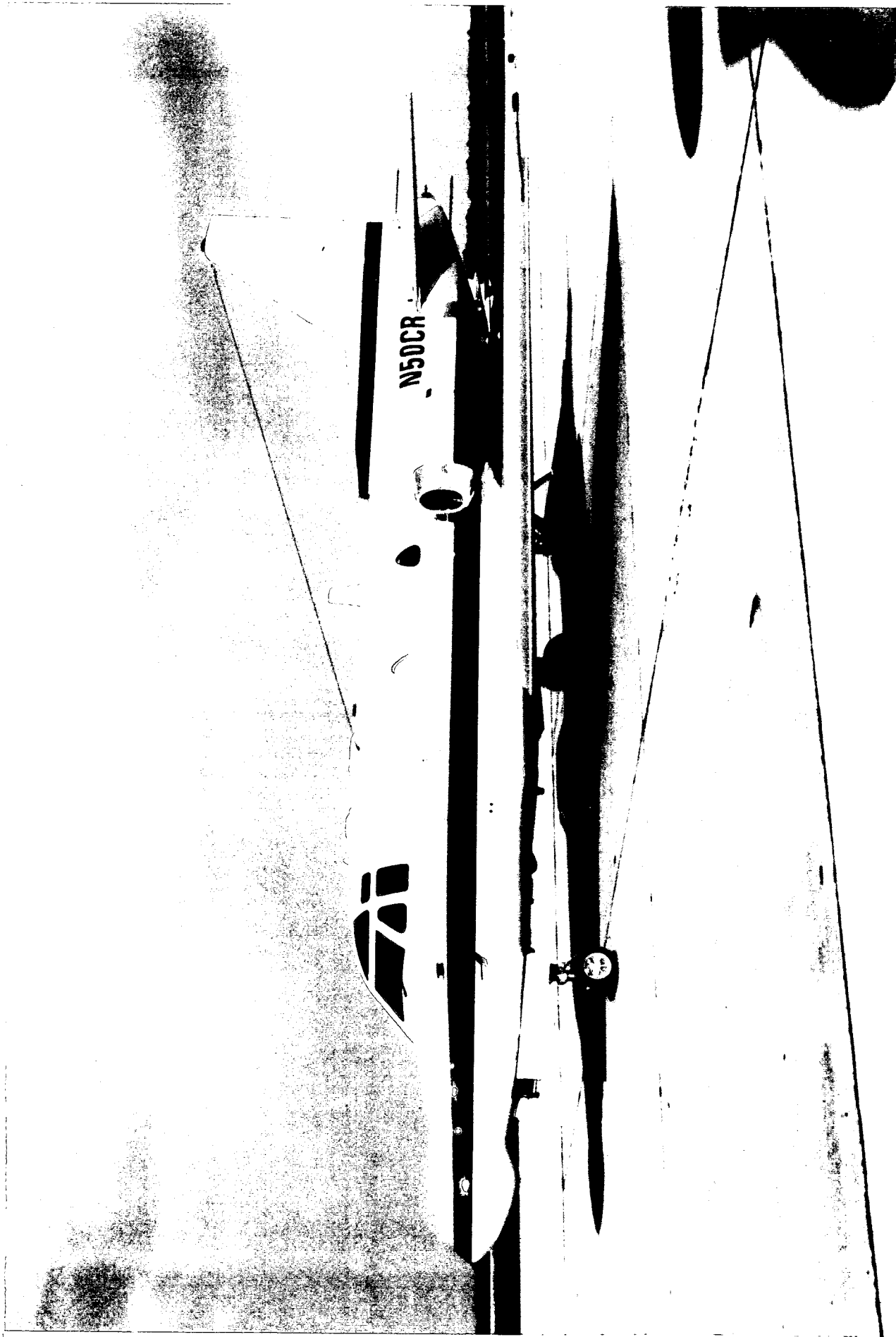


*Figure 5. Rockwell Collins Saberliner aircraft.*



## 4. DATA LINK AND COCKPIT DISPLAY

One of the key elements of the CWI program was to demonstrate the feasibility of a cockpit display for TDWR wind shear warnings. This task was first carried out in 1990 with the UND aircraft and then in the two succeeding years with the NASA ATOPS aircraft. A cockpit display was not attempted with the avionics manufacturers due to the limited development time and other considerations. The following sections describe the data link methodology used to transmit the data to the aircraft and what display mechanism was used in the cockpit. For all of the data link testing, the TDWR microburst products were generated from prototype wind shear detection algorithms and transmitted to the aircraft.

### 4.1. UNIVERSITY OF NORTH DAKOTA CESSNA CITATION II

The TDWR data was transmitted in real time from the TDWR testbed to the UND Citation aircraft via a Dataradio packet radio system. For this demonstration, a Cockpit Display Server was written at Lincoln that ingested the TDWR products and converted the data into airport-centered coordinates and performed the necessary computations. The Cockpit Server was implemented in C on a Sun 3 workstation. The output of the server was an RS-232 serial data stream. The packet radio system consists of two Dataradio modems which accept RS-232 information and transmit packetized data at a 4800 Baud rate. Figure 6 demonstrates the organization of the data link to the aircraft.

The cockpit display provided to the UND crew was a small monochrome CRT display that was capable of showing TDWR microburst, gust front, and storm cell information. The cockpit

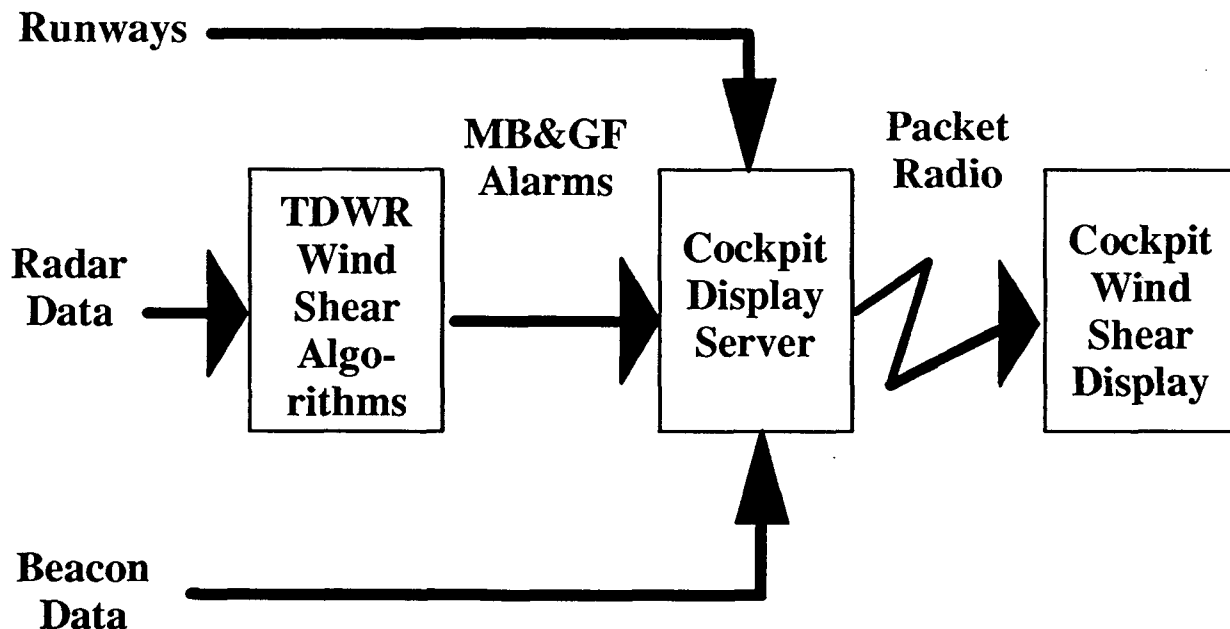


Figure 6. University of North Dakota data link system.

display is shown in Figure 7. The display is in "ARR" mode with a 30-knot microburst on the arrival corridors to runways 17 and 18. This unit is an Electronic Airborne Multipurpose Electronic Display (EAMED) from Eventide Avionics, and it is a modified version of the Argus 5000 Moving Map Display. The EAMED unit contains a monochrome CRT with an active area of 1.7 inches in width x 2.3 inches in height and a resolution of 256 x 512 pixels. The unit included a 6800 processor, two RS-232 serial ports, and four front panel buttons. The unit was 10 inches long and fitted in a standard three-inch instrument panel cutout.

The display was centered on the airport reference point and was oriented to magnetic north. Microbursts and gust fronts were depicted graphically, and the aircraft's own position was shown with the airport runway locations. The unit was capable of displaying the textual warnings generated by the TDWR algorithms on the bottom of the display. These textual messages could be generated for either the approach or departure ends of the runways.

The display was similar to that of the TDWR GSD that the tower supervisor uses. Microbursts were depicted as racetrack shapes, with the strength of the microburst displayed in the center of the microburst shape. If the microburst loss was less than 30 knots, it was an unfilled icon; if the loss was greater than or equal to 30 knots, the icon was filled in. Gust fronts were depicted as solid lines with the gain value drawn near the front. The textual messages at the bottom of the display were similar to the alphanumerical alerts that the individual tower controllers have available to read to incoming/departing pilots.

The UND display contained two additional products not available at the controller's position or at the supervisor's GSD. An experimental microburst prediction product was displayed, that showed dashed circles where microbursts were predicted. Also, the display was capable of displaying information on storm cells present within the terminal area. The areas of low and moderate reflectivity could be displayed by rectangular stipple patterns, with higher reflectivities denoted as a "C" on the display.

All of the above display options could be chosen with four buttons on the display ("ARR," "DEP," "ENR," and "AUX"). The "ARR" button allows the user to choose all arrival messages from the TDWR textual messages within a five nautical mile range around the airport. The "DEP" button allows the user to choose all alphanumerical alerts for aircraft on departure within a five nautical mile range around the airport. When the "ENR" button was chosen, a maximum range of the display is 15 nautical mile in the north-south direction, and 12 nautical miles east-west. The textual message would be disabled in this mode. Finally, if the user pressed the "AUX" button, the storm cell information would be displayed until the next screen update.

The cockpit display did not become operational until after the UND aircraft began operating in Orlando. The display became operational on July 11th and remained operational throughout the rest of the UND flights conducted under TDWR coverage. A total of six days of significant microburst activity occurred while the cockpit display was operational.

#### **4.2. NASA LANGLEY RESEARCH CENTER ATOPS B737**

During the summers of 1991 and 1992, TDWR microburst information was data linked to the NASA ATOPS aircraft. This was accomplished by processing the data at the TDWR testbed, then sending the data via telephone modem to the NASA site facility at MCO. Finally, a VHF packet radio was used by the NASA facility to transmit the data to the aircraft.

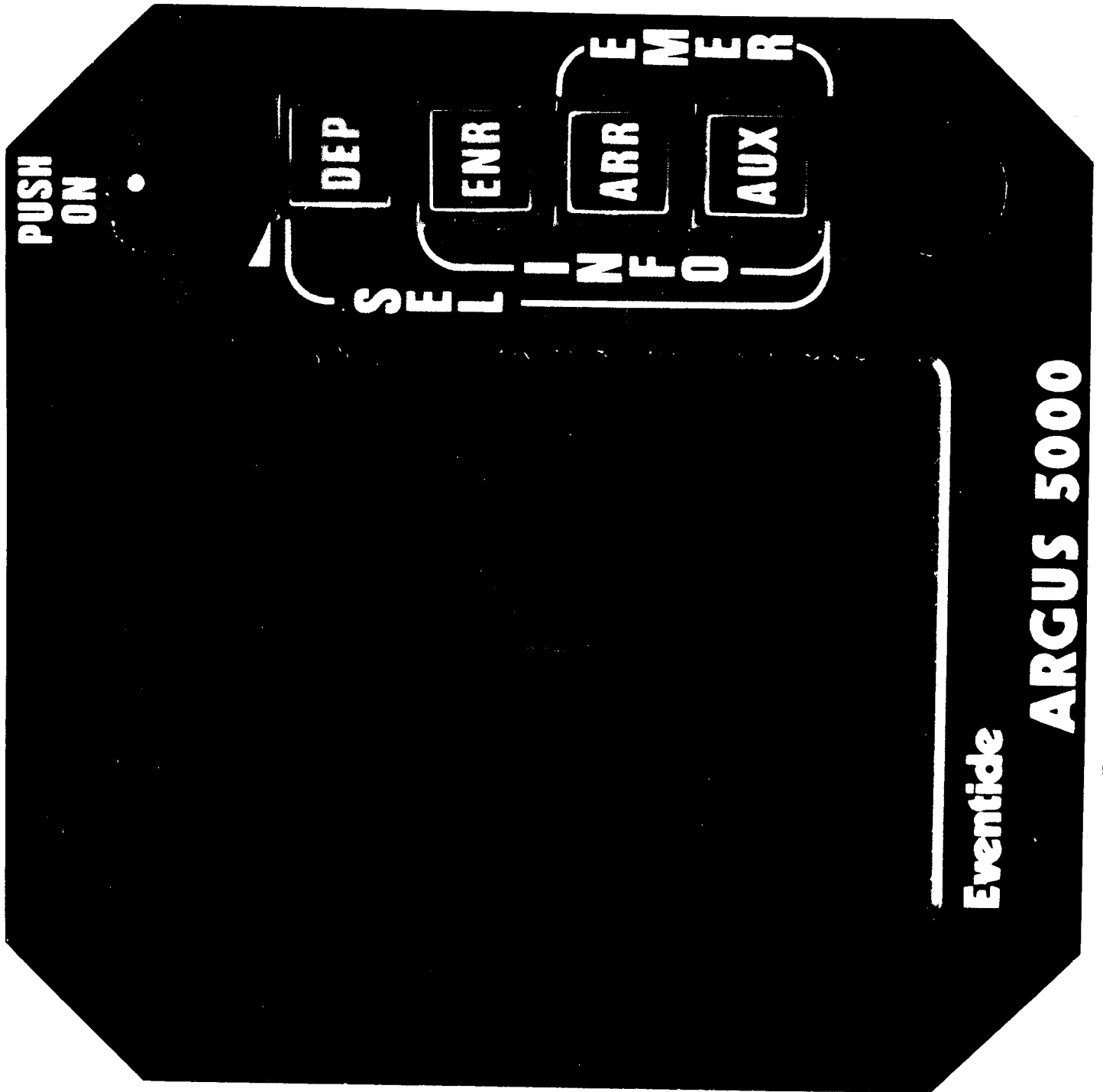


Figure 7. University of North Dakota cockpit display.



During the summer of the 1991, all microburst information was data linked to the NASA aircraft along with a waypoint indicating the region of strongest shear. The waypoint was manually inserted by an operator at the TDWR testbed radar. The NASA Cockpit Server converted all of the information into a special ASCII format. Then this data was sent to the NASA airport site for data link to the aircraft. During the summer of 1992 the Cockpit Server also collected precipitation information from the TDWR radar and sent this to the NASA airport site for data link to the aircraft. The data link and cockpit display used by the NASA aircraft are depicted in Figure 8.

The ATOPS aircraft was equipped with a color display that was capable of showing the TDWR microburst shapes in color and the current waypoint in an aircraft-centered frame of reference. On-board processing calculated a hazard index, called the F factor, for each shape as described in Section 5. Finally, on the moving map display, all microbursts were shown in a color-coded display. The microburst shape would be outlined in white if the F factor were less than 0.1, in orange if the F factor were greater than or equal to 0.1 but less than 0.15, and in red if the F factor were greater than or equal to 0.15. The moving map would display the loss value and F factor for one shape at a time and commutated over all shapes on the display.

The data link display worked reliably for the entire NASA demonstration in Orlando. This was facilitated by the placement of the radio antenna on top of a ramp lighting post at the NASA airport site. Also, the NASA VHF packet radio system performed much better than the system supplied for the UND demonstration.

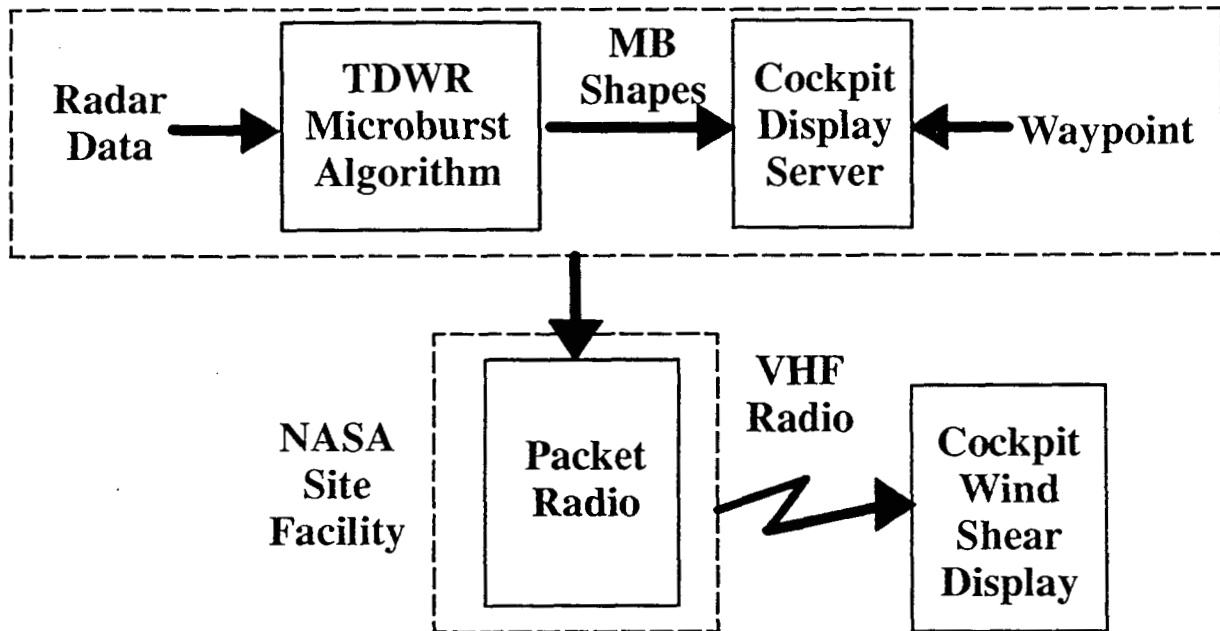
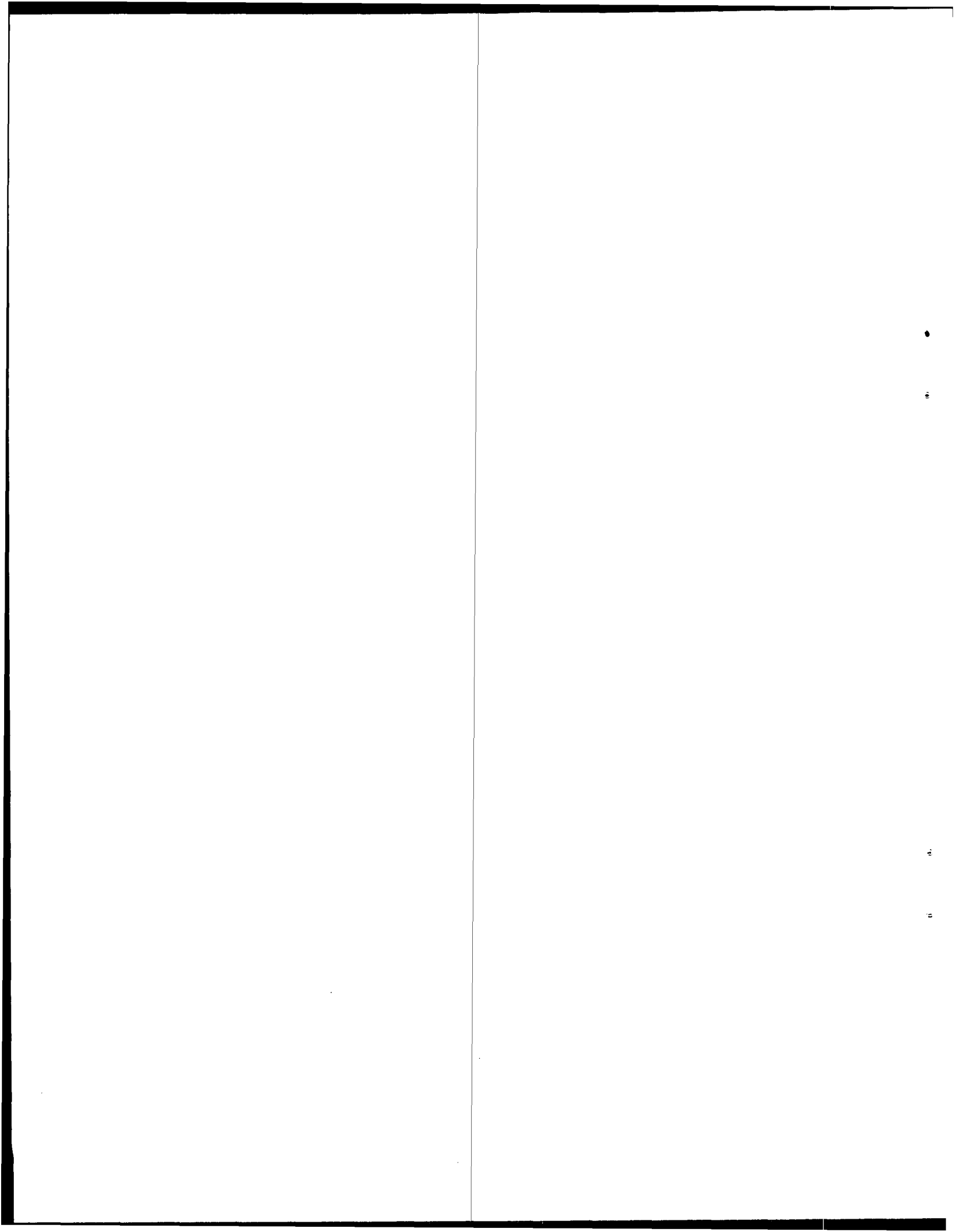


Figure 8. NASA ATOPS data link system.



## 5. DATA PROCESSING

The data used in the F factor comparison in Section 6 came from four different research aircraft mentioned previously and from the TDWR testbed at MCO. The data provided by the four aircraft research teams differed from each other in both content and format and needed to be put into a common format before use. The ground-based radar base data were not directly comparable to those gathered by any of the aircraft. Therefore, the radar base data needed to be processed to allow a comparison of hazard index. The first method involved the use of the testbed TDWR algorithm output, and the second involved a shear calculation from the radial velocity data. Fortunately, techniques are available that allow the calculation of F factor from each of these very different sources of data. For each aircraft, the F factor measurements were processed in an attempt to resemble the time-averaged F factor computed aboard the NASA aircraft.

The basic purpose of the data reduction effort was to convert each data source into a time-ordered set of F factor magnitudes along the aircraft's flight path. This process was repeated for each microburst penetration to yield the F factor estimate for each data source. The various estimates were then compared to one another using the aircraft-based figures as the truth values. Figure 9 is a graphical representation of the data processing approach taken to performing the analysis.

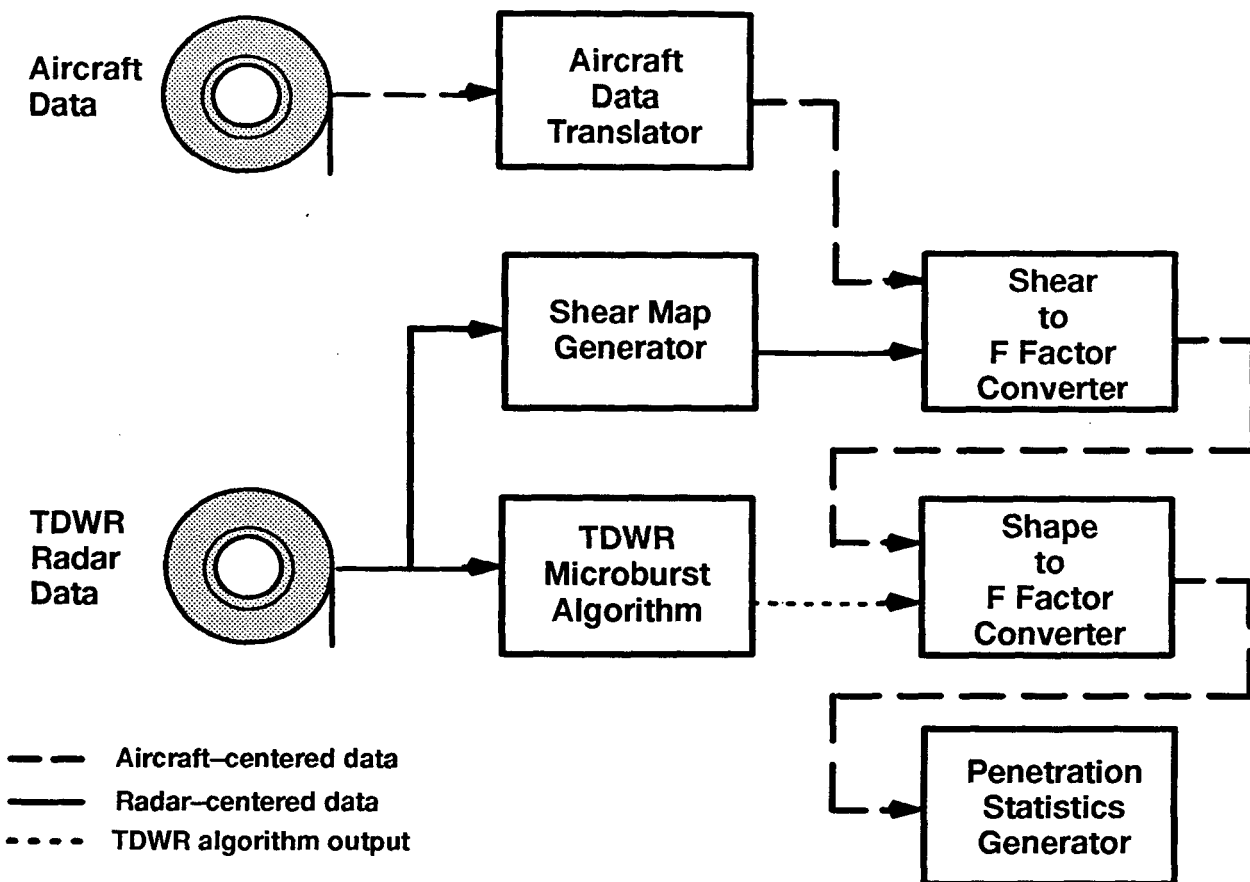


*Figure 9. Data processing overview.*

Before work could begin on F factor comparison, several C based programs were written to convert the data into a common format known as the aircraft state archive. This archive is composed of pertinent information about aircraft position, winds, and other aircraft centered fields. Also contained in this archive are fields for ground-based F factor estimates. Due to the variation in data recording methods aboard each aircraft and differences in database formats, several C based data reduction programs were written to convert each aircraft's database into the Lincoln aircraft state archive.

### 5.1. UNIVERSITY OF NORTH DAKOTA CESSNA CITATION II

The University of North Dakota Cessna Citation II aircraft data was provided to Lincoln in a 1 Hz resolution. The unfiltered raw aircraft data was recorded with the highly sensitive meteorological instrumentation aboard the aircraft. Normally, the *in situ* F factor is computed from the three-axis accelerometer data, however, in the case of the UND aircraft, a wind-based F factor was computed due to the lack of the three-axis accelerometer data.

F factor magnitude can vary widely for a given storm penetration depending on the filtering applied during its calculation. The basic definition of F factor makes no distinction between high spatial frequency components (perceived as turbulence) and the low-frequency components that compose the actual performance-loss threat to an aircraft. For transport-class aircraft, it has been determined that shears on a scale of one to three kilometers pose the greatest threat (Lewis, 1994). The University of North Dakota Cessna Citation II wind-based F factors presented in this report were produced using winds that had been put through a simple six-second moving average filter. The results generated using this method were compared with NASA's accelerometer-based reactive algorithm, and the two methods yielded peak F factor values that were within five percent of each other for several representative microburst flights. The equations are presented below, along with the discrete approximations used to generate the hazard index from sampled data:

$$F_h = dW_h/dt / g \approx \left\{ \left( \sum_{i=0}^5 W_{hi} / 6dt \right) - \left( \sum_{i=6}^{11} W_{hi} / 6dt \right) \right\} / g \quad (5.1)$$

$$F_z = \left( \sum_{i=0}^5 W_{zi} / 6dt \right) / TAS_{i=0} \quad (5.2)$$

Where  $W_h$  is the along-track component of the horizontal wind field. The sample interval,  $dt$ , was one second. The six-second smoothing combined with the six-second delta used in the derivative calculation resulted in a shear calculation over a distance of approximately one kilometer at the air speeds typical during the microburst penetrations.

The simple wind-based F factor algorithm described above has a major shortcoming that had to be kept in mind when selecting appropriate flight data for analysis: aircraft maneuvering can introduce artifacts in the results. One can imagine a large turn initiated in a steady crosswind. The results would be indistinguishable from those obtained from a genuine wind shear. Air flow disturbances around the pressure ports also can give misleading wind field indications during deviations from level flight. Many of these problems can be overcome with sufficiently sophisticated post processing, but the lack of three-axis accelerometer data for the UND data precluded this. The solution was to trim down the times of interest to include only relatively straight and

level flight. The UND flight crew, in general, lined up on a radar radial prior to entering a microburst and flew straight through it, so this pruning of the penetrations for straight and level flight cost relatively little in terms of lost data.

Several problems were noted in processing the UND data. The instrumentation navigation system (INS) unit used on the UND Citation aircraft was prone to drift error as much as a kilometer or two after prolonged periods of complex maneuvering. Also, occasional glitches in the Citation instrumentation system caused erroneous data to be recorded.

The INS drift correction problem was solved by using the VHF Omni Range/Distance Measuring Equipment (VOR/DME) data to correct for long-term drift. This correction turned out to be more complicated than initially imagined since the VOR/DME data was incorrect whenever the aircraft was near the ground or whenever the Area Navigation (RNAV) system was switched to ILS mode. Ultimately, it was decided to use the VOR/DME data only if the correction seemed plausible (i.e., within a few km).

To correct the problems in the Citation instrumentation, a capability was added to correct for biases or errors in the recorded data. Currently, bias correction can be applied to the aircraft position and altitude over specific time periods. This allows drift corrections to be applied on days where the VOR/DME data is not usable (e.g., July 7th). It also allows an altitude bias to be removed on July 7th data.

## **5.2. NASA LANGLEY RESEARCH CENTER ATOPS B737**

The NASA B737 data was provided to Lincoln after post-flight data quality checking was performed by NASA Langley. This post processed data ensured that all of the data provided to Lincoln did not require any filtering or data correction. However, the ASCII files provided by Langley needed to be converted to the Lincoln aircraft state archive. This was performed in a C based program. The NASA data contained location, altitude, *in situ* winds, and F factor as well as other meteorological measurements crucial for wind shear detection.

## **5.3. AVIONICS MANUFACTURERS**

Three avionics manufacturers flew during the summers of 1991 and 1992. Due to the limited equipage on the Bendix aircraft and on board the Westinghouse aircraft during the summer of 1991, this data was not converted into the aircraft state archive. Westinghouse increased the *in situ* equipment over the winter of 1992 and was properly equipped during the summer of 1992. Rockwell Collins Corporation flew during the summers of 1991 and 1992. Rockwell's Saberliner was properly equipped for *in situ* measurements. Each of the manufacturers provided Lincoln with a simplified form of their aircraft *in situ* data that were converted to the Lincoln aircraft state archive.

## **5.4. TERMINAL DOPPLER WEATHER RADAR**

The TDWR system consists of a single Doppler radar that can only directly sense the radial component of the wind field in a storm, which leads one to question its utility for detecting a phenomenon that is, by nature, three dimensional. At this time it might be useful to examine a few reasons that might lead one to believe that a single radar can be successful at remotely sensing wind shear hazards.

The most effective way to enhance the utility of a single Doppler radar is to situate it properly. This is a major issue for the TDWR project, and great effort has been expended to place the

radars where their beams are nearly parallel to the airport's most frequently used runways. During the research flights presented here, many of the penetrations were undertaken over MCO along the normal approach and departure paths. When off-airport storm penetrations were undertaken, the flight paths chosen were generally located along the radial of the radar. The relevant horizontal wind component in an F factor calculation is the one that lies along the flight path. Therefore, if the flight path and the radar's radial are coincident, no data is lost in the horizontal plane.

#### 5.4.1. TDWR Microburst Algorithm

The TDWR microburst algorithm defines a microburst outflow region by fitting a number of racetrack-shaped icon figures around groups of radar radial velocity segments that show sufficient shear along their length, as shown in Figure 10. Site-adaptable parameters can be selected to break a single icon (also referred to as a "microburst shape") into smaller subsections. In the current algorithm, each icon is assigned a value denoting the highest peak-to-peak velocity difference found in all the segments contained in that shape. The Lincoln implementation of the microburst algorithm outputs a shear estimate that represents the *average* shear across one of the highest-loss radial segments.

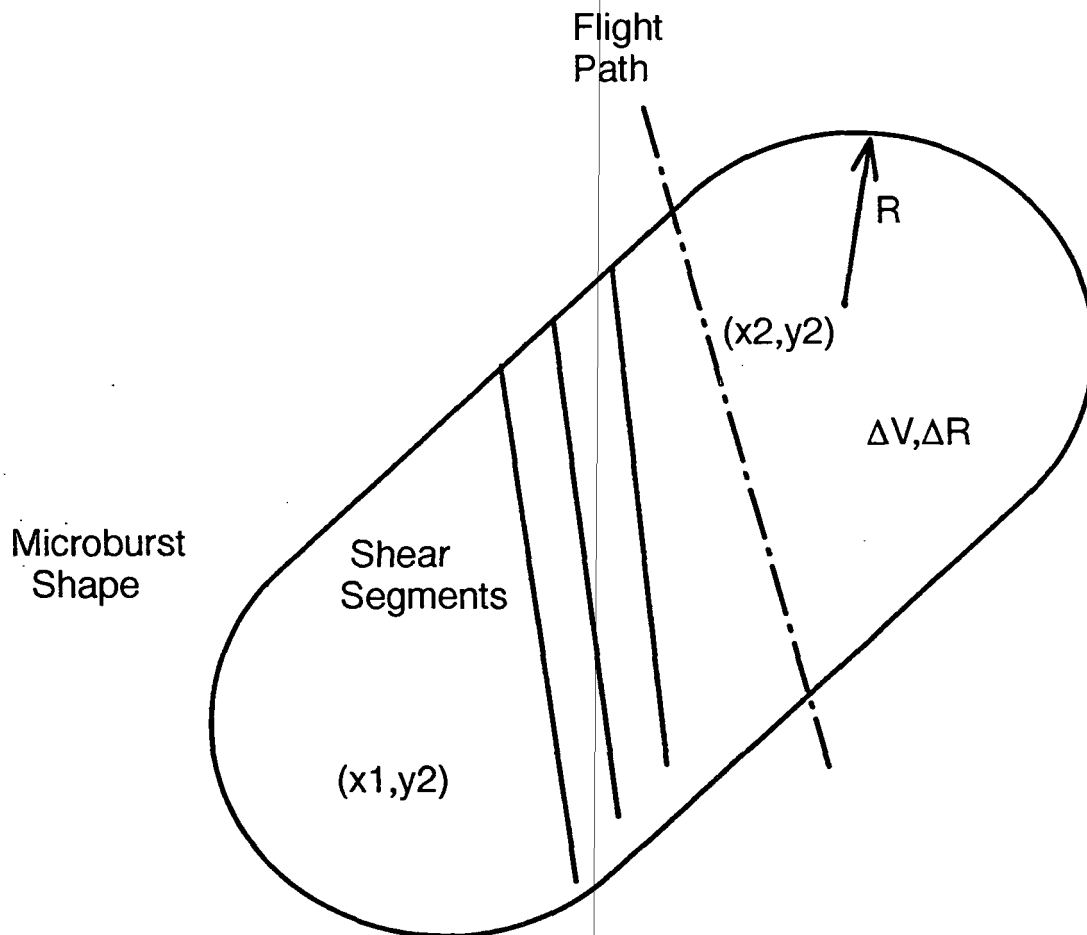


Figure 10. Illustration of a microburst shape from shear segments.

A small study was undertaken using only the UND data set to determine the sensitivity of the F factor to different methods of calculating average shear. The Lincoln implementation of the TDWR microburst algorithm can be configured to calculate the  $\Delta V$  and  $\Delta R$  values in several different ways. Four different techniques were evaluated: using the peak loss segment's shear value, the segments with the 50th and 85th percentile shear, and the average segment shear. The result of comparing the correlation between the TDWR and aircraft F factor using these four different techniques indicated that the 85th percentile shear values were clearly superior for use in calculating TDWR F factor from microburst alarms. The 85th percentile value was used for the remainder of the processing, and all results presented here were generated using this technique.

An algorithm that is intended to convert the microburst algorithm's average shear output into an estimate of the peak F factor present in the storm must estimate the downdraft velocity present in the microburst. This can be done by using a slightly modified version of the (Bowles, 1990) formula:

$$F = K' (\Delta V / \Delta R) (GS/g + 2h/TAS) \quad (5.3)$$

where  $\Delta V$  is the alarm's loss value as reported by the TDWR,  $\Delta R$  is the distance over which the reported loss occurred, GS is the ground speed of the aircraft, TAS is its true air speed, and h is the height of the TDWR antenna beam at the alarm position.

$K'$  in equation (5.3) attempts to estimate a one-kilometer average shear, centered at the microburst core, in a least-squares sense, using known TDWR data and analytical wind shear profiles. The term's value is a function of  $\Delta R$  and a "distance of interest" over which a least-squares fit had been determined for the shear in an analytic microburst model.

The modified Bowles formula estimates the downdraft velocity in the second term of equation (5.3) by employing a simplified model of the mass continuity exhibited by the microburst. The outflow region is viewed as a cylinder, shown in Figure 11, with the ground acting to prevent outflow at the bottom. Therefore, what flows into the top (i.e., downdraft) must exit through the sides of the cylinder as horizontal outflow. This suggests that the outflow is directly proportional to the downdraft.

The software also accommodated several methods for attempting to compensate for the discrepancy between the TDWR radar beam height and the aircraft altitude at the microburst location. The data was processed and analyzed separately for each alternate form of the equation. The details and results of the various refinements to the estimation techniques are discussed in Section 6.5.

The first processing runs to convert the TDWR microburst alarm values into F factors were performed by taking the actual output archives from the TDWR operational demonstration and plugging them into equation (5.3). The computer program that performed the calculations accepted the aircraft data archive as well as the TDWR algorithm output. This design enabled the TDWR F factors to reflect the actual ground and true air speed of the research plane. The program took each aircraft record, selected the most recent microburst alarms from the TDWR archive, and searched for any alarm region that coincided with the location of the aircraft at that time. Certain cases occurred where the aircraft traversed space in which multiple, overlapped

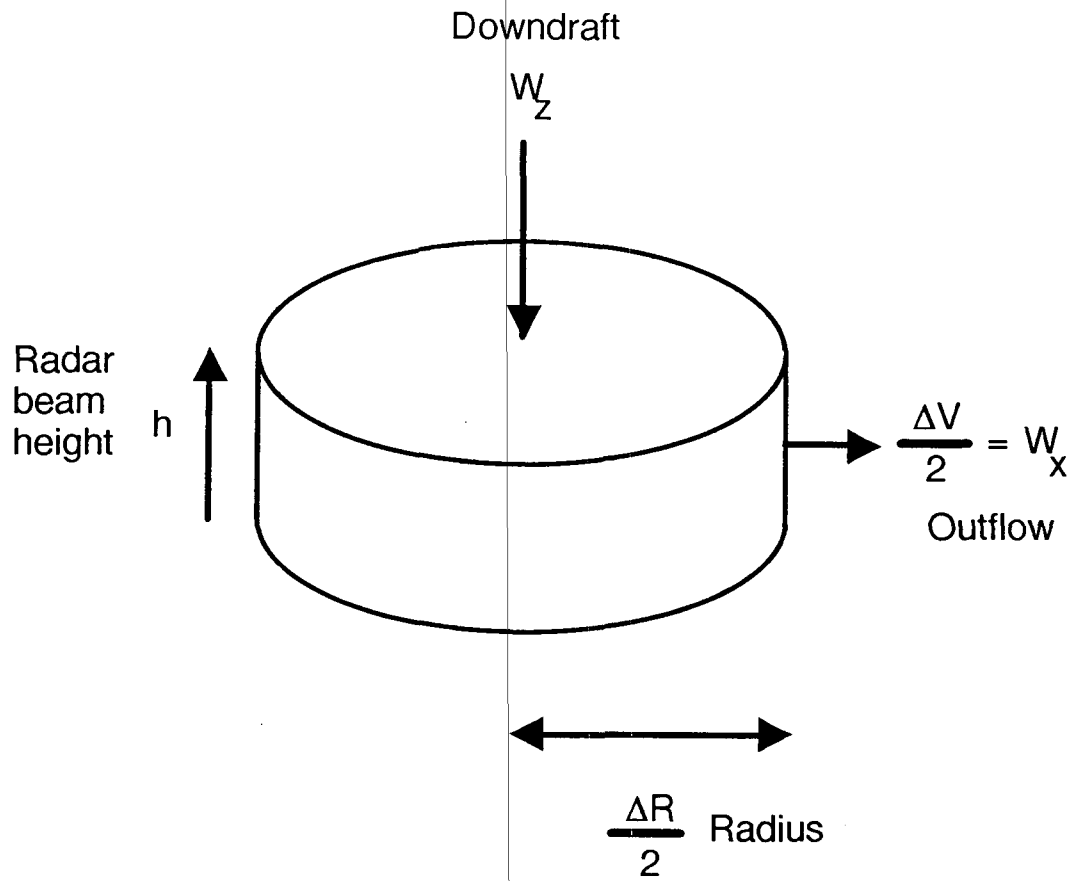


Figure 11. Illustration of microburst continuity.

alarm regions existed. In those cases, the recorded value was from the region with the highest F factor.

It became evident at an early stage in the study that the quality of the F factor estimations could be improved by changing some of the microburst algorithm's site-adaptable parameters to values different than those used in the 1990 operational demonstration. The data processing regimen was thus revised to include the regeneration of the microburst alarms from the raw inputs used by the algorithm, which allowed a consistent set of parameters to be used for both 1990 and 1991 data.

#### 5.4.2. TDWR Shear Map

F factors were calculated from the Lincoln TDWR testbed's radial velocity data in several steps. The radar's velocity, reflectivity, and signal-to-noise ratio values were archived onto magnetic tape throughout the course of the TDWR operational demonstration. This raw data was run through a suite of data quality enhancement algorithms: point target removal, range obscuration editing, and clutter filtering. This Data Quality Edited (DQE) information recreated, with

the omission of velocity dealiasing, the same data stream that was made available to the TDWR algorithms in real time.

The edited radar data was used as input to a program that calculated a map of the radial shear from the radial wind velocity values. The data was first subjected to a velocity dealiasing algorithm developed at the National Severe Storms Laboratory (NSSL) and then to a range-adaptive median filter that nominally operated on 500 x 500 meter rectangles. The radar's gate spacing is 150 meters; its beamwidth is 0.5 degrees, with radials spaced one degree apart. The median filter was constrained to use an odd number of data points (between 1 and 7) in the azimuthal direction, rounding upward as necessary. With these parameters, the filter size varied from 3 gates-by-7 radials close to the radar to 3 gates-by-3 radials at 20 km from the radar. The actual shear computation for each range gate was made by performing an unweighted least-squares fit on seven gates centered about the point of interest. With the TDWR radar's 150-meter gate spacing, this resulted in a fit over a radial distance of 1050 meters. Figure 12 is a depiction of a simple case of using the least-squares fit in the shear computation. This general method of shear computation is similar to work done by Charles Britt(1992) of Research Triangle Institute for NASA's airborne Doppler wind shear detection system.

The F factor was calculated from the shear data by taking the shear at the point in space closest to the aircraft at any given moment and combining that with the plane's ground speed and air speed. The calculation was similar to that used for generating F factor estimates from TDWR microburst alarms:

$$F = (dV/dR) ( V_g/g + 2h/V ). \quad (5.4)$$

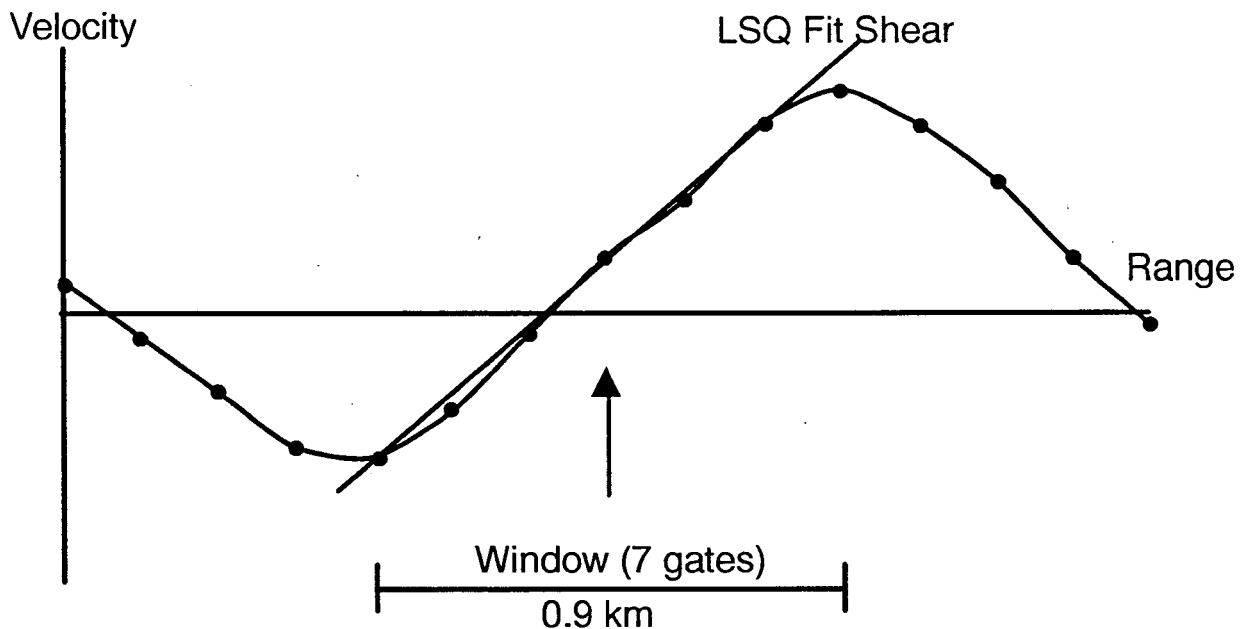


Figure 12. Least-squares-fit shear computation.

Note that this equation differs from equation (5.3) in the omission of the  $K'$  term. In that equation,  $K'$  attempts to predict the shear (at the center of an "ideal" microburst) based on the gross measurements of size and differential velocity provided by the TDWR microburst algorithm. This estimation technique is neither needed nor applicable in the present case, as the  $(dV/dR)$  term supplied by the shear map program already represents an estimate of the shear centered about the point of interest and thus can be used directly.

## 5.5. INTEGRATED TERMINAL WEATHER SYSTEM

As its primary data source, the ITWS microburst detection algorithm uses the shear map data from the TDWR base data, as discussed in the previous section. It operates by locating segments of radial shear with an average shear above defined threshold levels (Dasey, 1993). Currently, the algorithm thresholds at four shear intervals (4.0, 6.0, 8.0, and 10.0 m/s/km). These segments are constrained to avoid containing too many bad data points or negative shear values. Then for each threshold level, segments on adjacent radials are associated with one another into regions of shear. For each region a loss value is determined from the radial velocity by taking a velocity difference between two points for which the average shear is above 2.5 m/s/km. Next, a circular shape is optimized to best fit the resulting regions and is tested for sufficient peak shear and loss for a wind shear alert (minimum 15 knots, 5.0 m/s/km) or a microburst alert (minimum 30 knots, 10.0 m/s/km).

One of the goals of the ITWS microburst detection algorithm is to more accurately characterize the strength, in terms of F factor, of a microburst. Estimation of F factor can be done for the ITWS algorithm by using the horizontal component of the F factor equation (5.4) and substituting the  $\Delta V/\Delta R$  term with the shear value of the microburst as detected by ITWS. Before doing this, an altitude compensation can be applied to the data, similar to that done when computing F factor from the TDWR shear map.

From equation (5.3), the vertical term can be calculated from estimates of microburst parameters from the ITWS algorithm using the following formula:

$$F = K' (\Delta V/D) (2h/TAS) . \quad (5.5)$$

where  $K'$  is a constant,  $\Delta V$  is the velocity difference,  $D$  is the diameter of the ITWS shape,  $TAS$  is the true air speed of the aircraft, and  $h$  is the height of the radar beam.

## 6. F FACTOR COMPARISON

### 6.1. F FACTOR ESTIMATES FROM TDWR MICROBURST ALGORITHM

For each of the 118 microburst penetrations, an F factor was calculated from the output of the Lincoln version of the TDWR microburst algorithm using the techniques described in Section 5.4.1. Figure 13 is a plot of the TDWR estimated total F factor (TDWR  $F_T$ ) compared to the *in situ* F factor. From the figure it can be seen that the computed TDWR  $F_T$  was consistently higher than the *in situ* F factor. Most notable is that the estimation was biased especially high for the NASA events.

The unexpectedly high values of TDWR  $F_T$  may be due to several factors, the most obvious of which is that the F factor computed from the microburst alarms assumes that the shear has a constant value at all points within the boundary of the microburst icon. This assumption is incorrect, and since the aircraft sampled only a small portion of the area enclosed by the microburst alarms, it is quite possible that on many occasions they missed the localized "hotspot" of shear that caused the large value reported by the TDWR.

### 6.2. F FACTOR ESTIMATES FROM TDWR SHEAR MAP

Figure 14 shows the peak total F factor as estimated from the TDWR shear map versus the peak total *in situ* F factor, as discussed in Section 5.4.2. A comparison with Figure 13 shows an

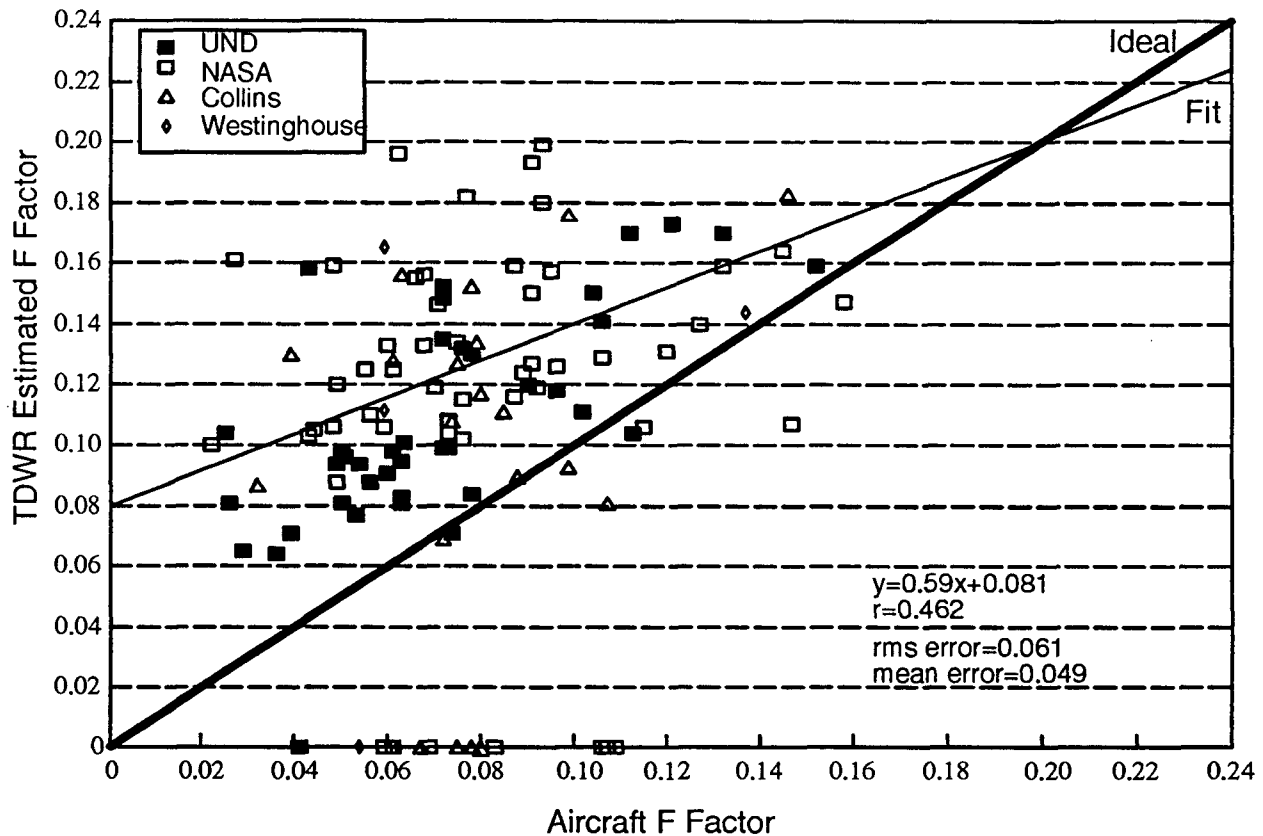


Figure 13. TDWR alarm vs. aircraft total F factor.

improved correlation between the TDWR and *in situ* F factor at the expense of an increased incidence of underestimation. Examination of the significant cases of underestimation reveals that in nearly all cases the error was due to the aircraft encountering a large downdraft that was not predicted by the shear map F factor calculation.

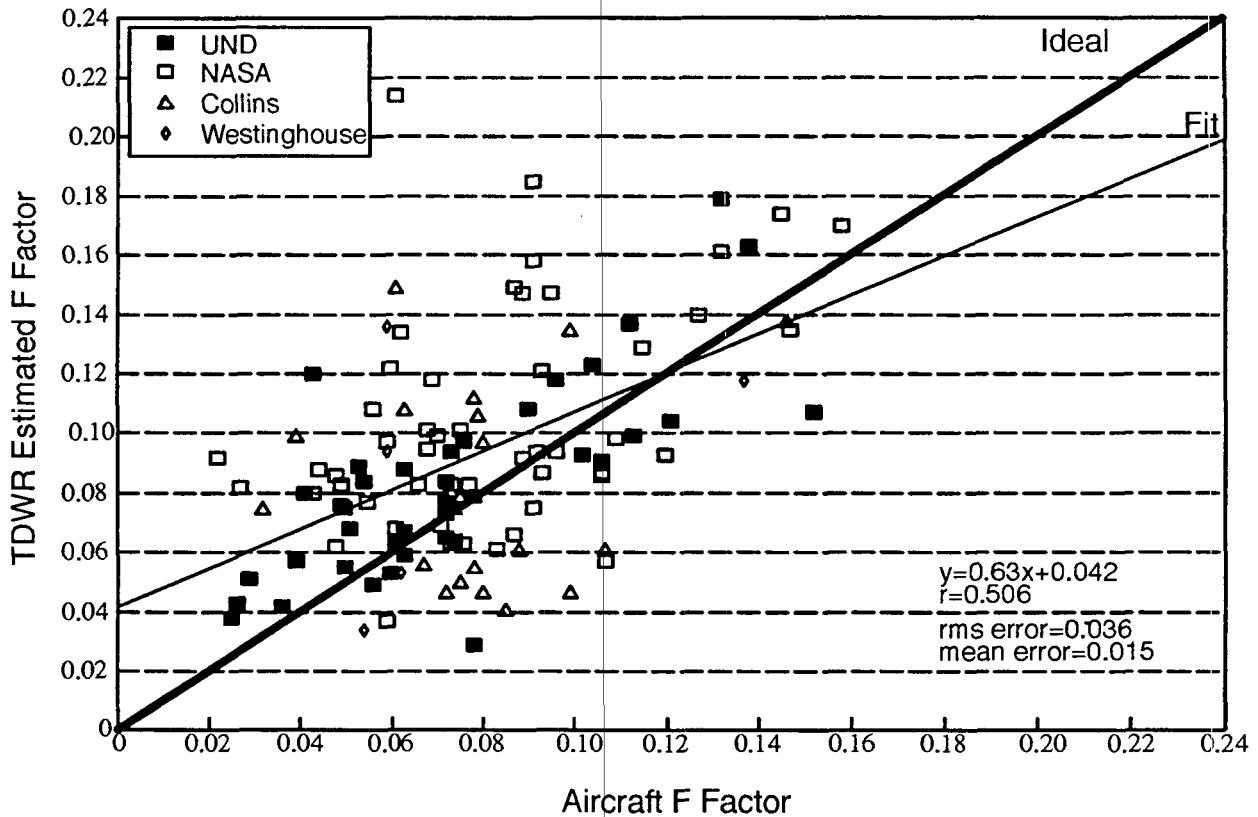


Figure 14. TDWR shear map vs. aircraft total F factor.

### 6.3. F FACTOR ESTIMATES USING ALTITUDE CORRECTION

A possible explanation for an overestimated F factor from the shear map is the difference between the altitude of the aircraft and the radar beam. Figure 15 shows the altitude of the aircraft penetration versus the altitude of the TDWR radar beam at the storm location. For most of the events, the aircraft penetrated the microburst at a much higher altitude than the radar beam. Physical observations and modeling results suggest that both horizontal shear and the downdraft velocity in a microburst vary with altitude. Thus, it would seem prudent to attempt to compensate for the discrepancy between the height at which the TDWR antenna beam and the aircraft measured the microburst intensity.

The Osguera & Bowles(1988) analytical microburst model includes a vertical shaping function for the horizontal wind velocity that is a good fit to experimental data. The function, whose shape is illustrated in Figure 16, depends only on altitude and was therefore a suitable choice as a means to correct for the altitude differences in the data set. The altitude-corrected shear map F factor was calculated by multiplying the measured shear by the ratio of the shaping function evaluated at the height of the TDWR beam and the aircraft penetration altitude. The modified shear value was then used as the input to both the horizontal and vertical F factor calculations.

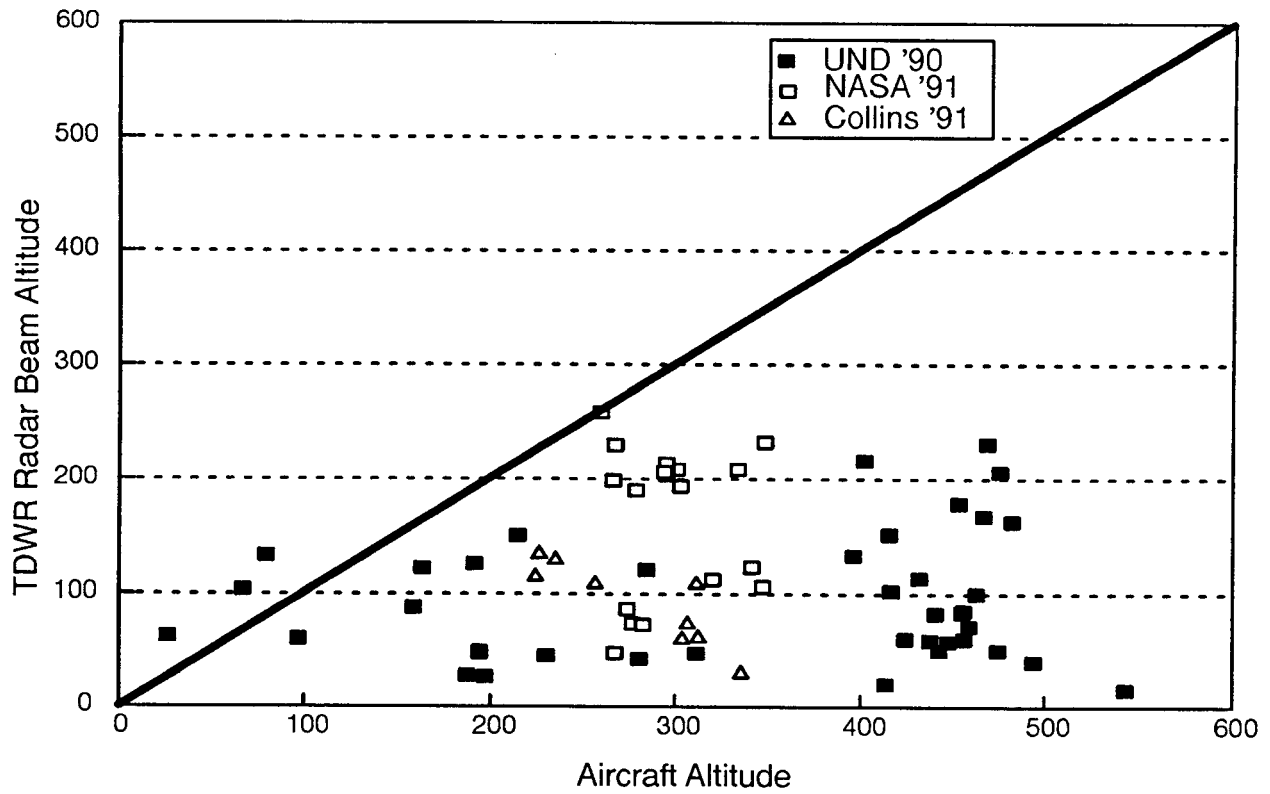


Figure 15. Comparison of aircraft altitude during microburst penetration and TDWR radar beam altitude.

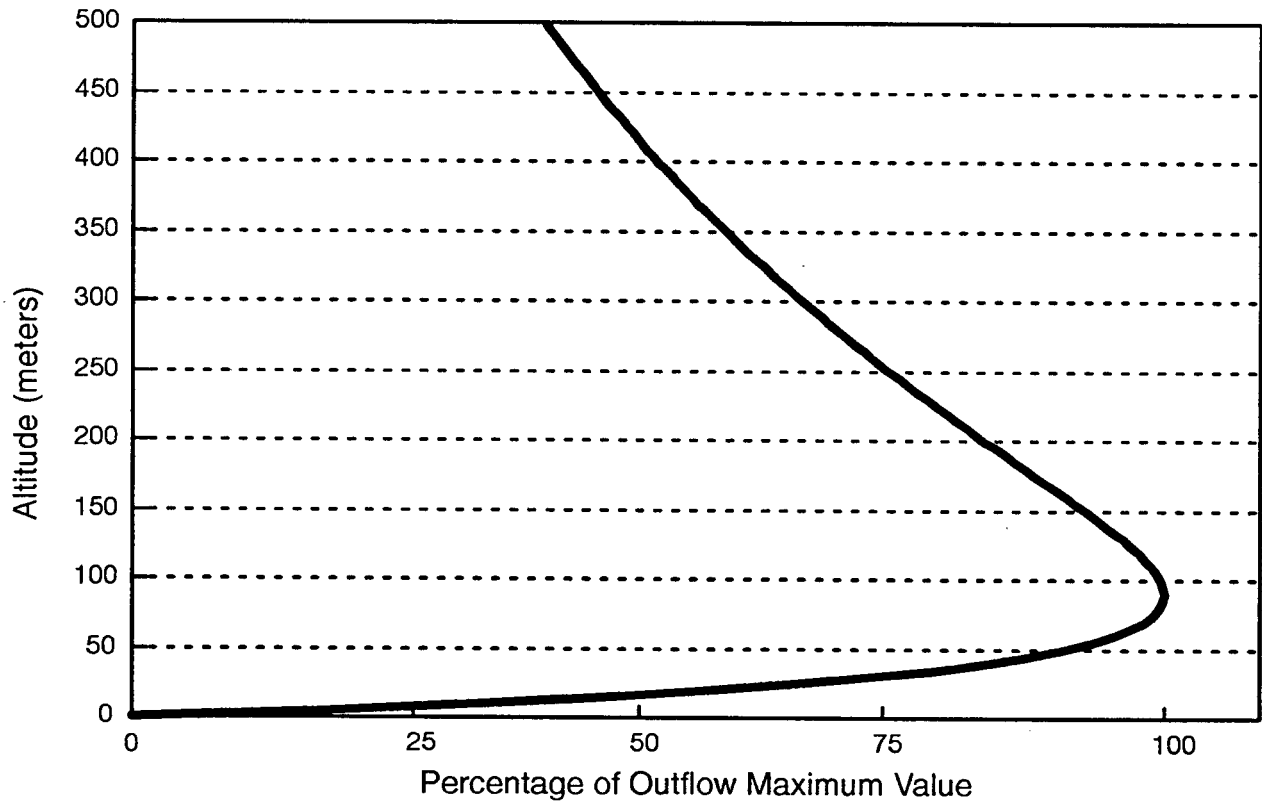


Figure 16. Altitude profile used in Oseguera & Bowles model.

It is important to note that the altitude profile used was developed from the Joint Airport Weather Studies (JAWS) data and is commonly accepted as the altitude profile for loss ( $\Delta V$ ). In a real microburst, it is possible that the vertical profile for F factor is rather different than that for loss due to an outflow diameter that varies with altitude.

Figure 17 is a comparison of the shear map total F factor after the altitude correction has been applied versus the *in situ* F factor. The height of the maximum outflow in the profile used was 90 meters as determined by the JAWS data sets. Although this method visually provides a better estimate of the F factor, the statistical measurements do not improve due to several cases of significant under- and overestimation. In several cases where an underestimation was due to a downdraft estimate that was already too low, the modified results were worse.

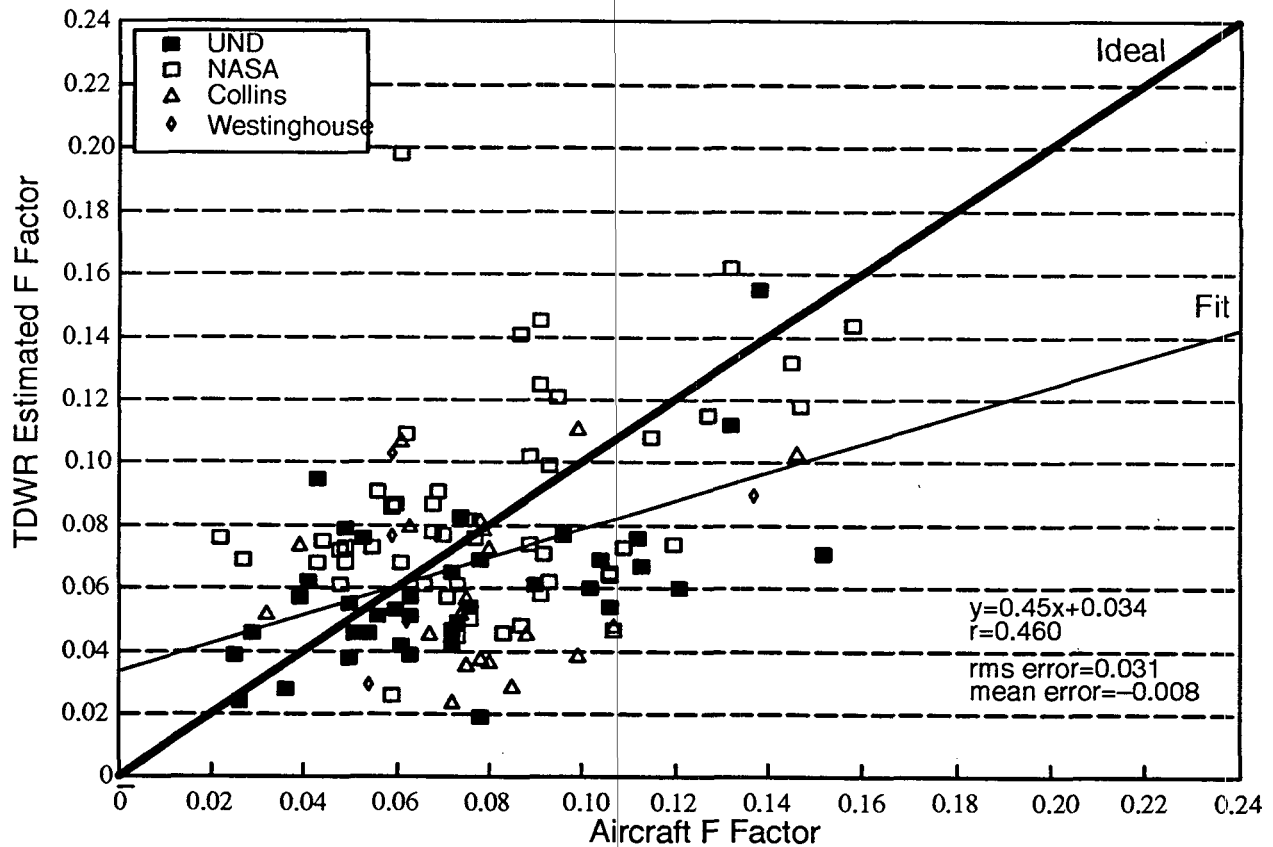


Figure 17. TDWR shear map vs. aircraft total F factor using altitude profile correction.

#### 6.4. ESTIMATING HORIZONTAL TERM OF F FACTOR

It is useful to look at the horizontal and vertical components of the F factor when attempting to analyze the success and failure of the various estimation techniques. The horizontal component can be calculated directly from the TDWR ground-based data using the following formula:

$$F_{\text{horizontal}} = (dV/dR)(GS/g) \quad (6.1)$$

Figure 18 shows that the horizontal component of the TDWR estimated F factor was overestimated in all cases in which the aircraft encountered a microburst alarm. This overwarning can be attributed to two factors. First, the aircraft did not encounter the region of strongest shear within the microburst alarm. Second, the aircraft penetrated the microburst at a higher altitude than the radar beam.

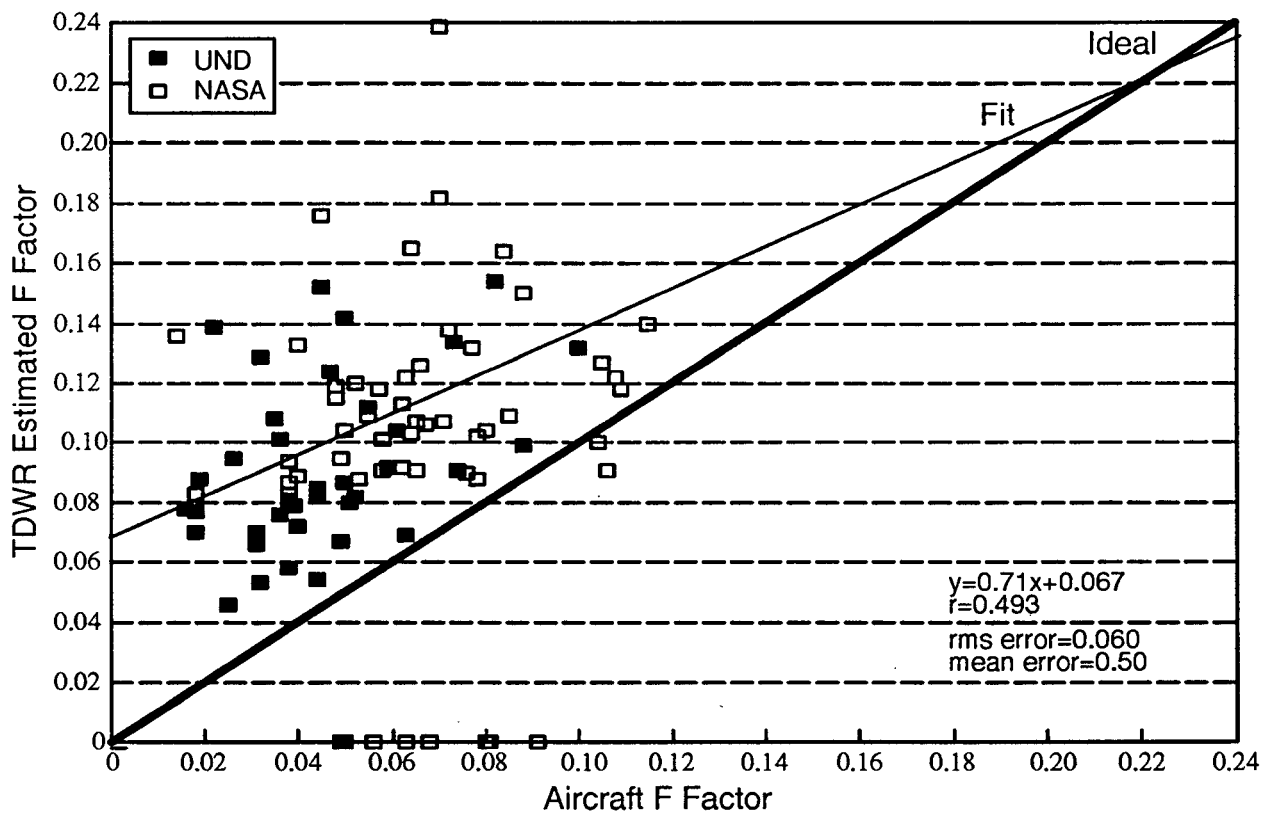


Figure 18. TDWR shape vs. aircraft horizontal F factor at F total peak time.

Figure 19 shows the horizontal component of the F factor as estimated from the shear map. This method provides a better estimate of the horizontal F factor, but some overestimation is still evident. Correcting for altitude, Figure 20 shows that there is a dramatic improvement in the shear map estimation for horizontal F factor. Therefore, using the shear map and correcting for altitude seems to provide an excellent estimation technique of the horizontal F factor, but what about the vertical component?

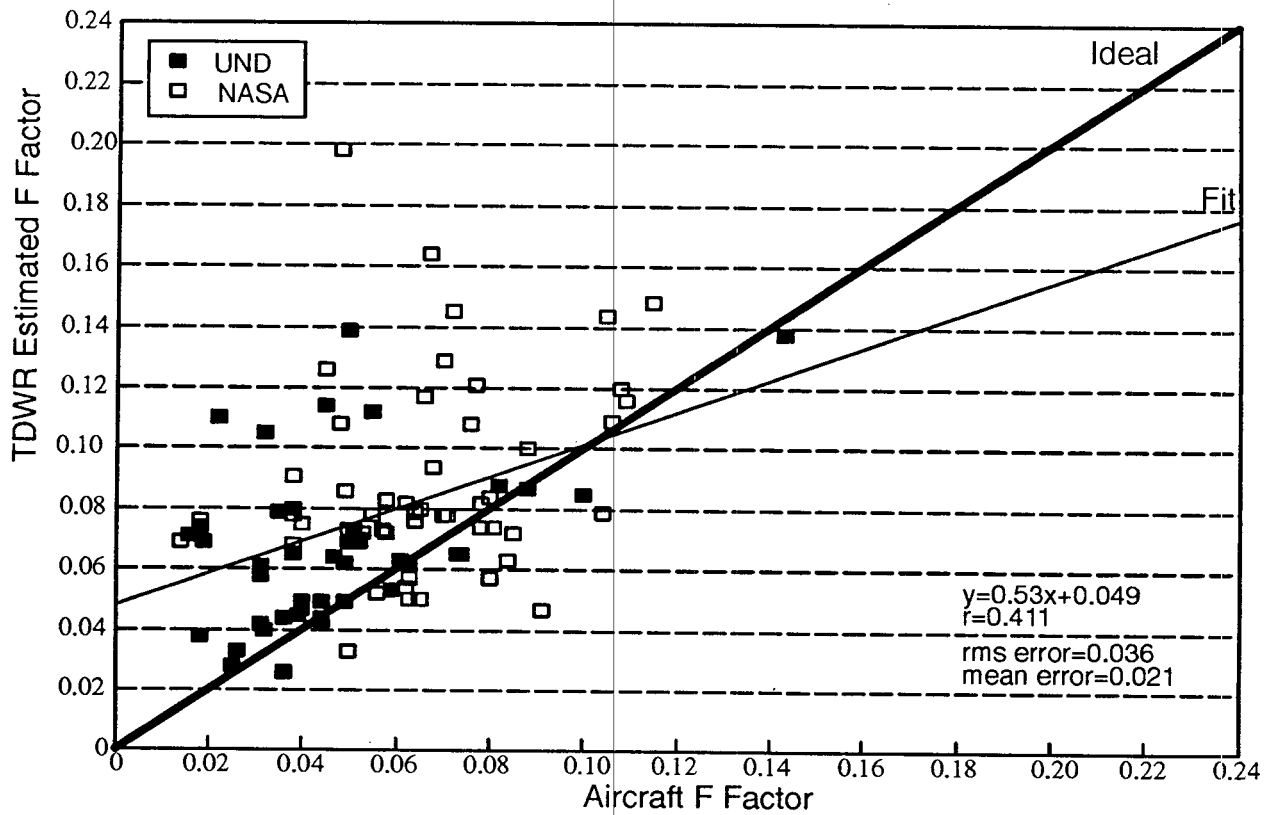


Figure 19. TDWR shear map vs. aircraft horizontal F factor at F total peak time.

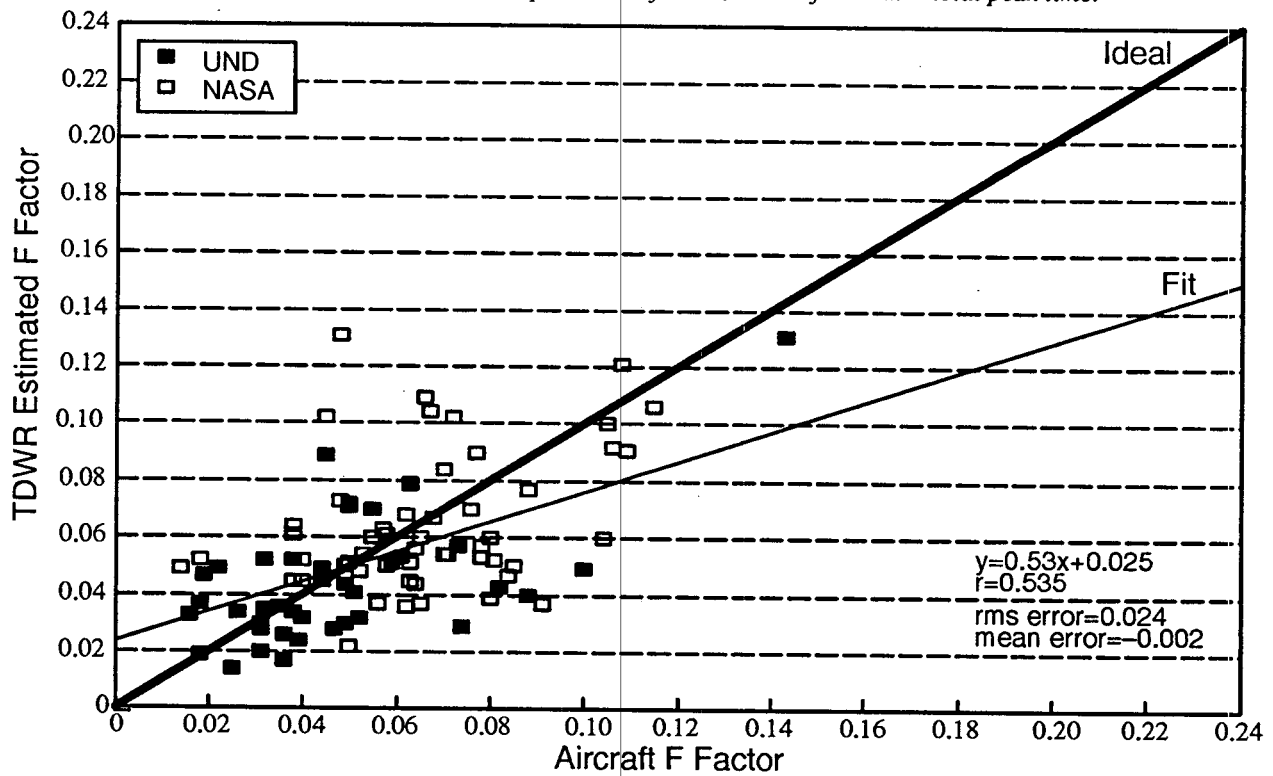


Figure 20. TDWR shear map vs. aircraft horizontal F factor at F total peak time using altitude profile correction.

## 6.5. ESTIMATING VERTICAL TERM OF F FACTOR

The vertical component of the F factor has been estimated in this research using the following formula:

$$F_{\text{vertical}} = (dV/dR)(2h/TAS) \quad (6.2)$$

This is the Bowles formula which attempts to predict the downdraft based on a measurement of the horizontal shear in a storm. Figure 21 shows the TDWR vertical F factor estimate using the microburst alarms versus the aircraft vertical F factor for all the UND and NASA events. From the figure it can be seen that the vertical estimation ranged from 0.0 to 0.04, while the *in situ* ranged from -0.01 to 0.09. Why did the *in situ* vertical F factor cover such a wide range while the estimated vertical F factor did not?

A probable explanation for the poor performance of the downdraft estimation used in this research can be found in Figure 22. The figure depicts the variation in downdraft velocity across the radius of a microburst. This horizontal shaping function has been proposed by Vicroy(1991) as an improvement to the original Oseguera & Bowles model (Oseguera & Bowles, 1988). The figure shows that the peak downdraft occurs only at the center of the microburst, with the downdraft velocity decreasing in magnitude (and eventually turning into an updraft) toward the edge of the event.

The vertical F factor estimation given by equation (6.2) is valid only in the core of a microburst. For many of the cases in the study the aircraft penetrated the edge, not the core of the mi-

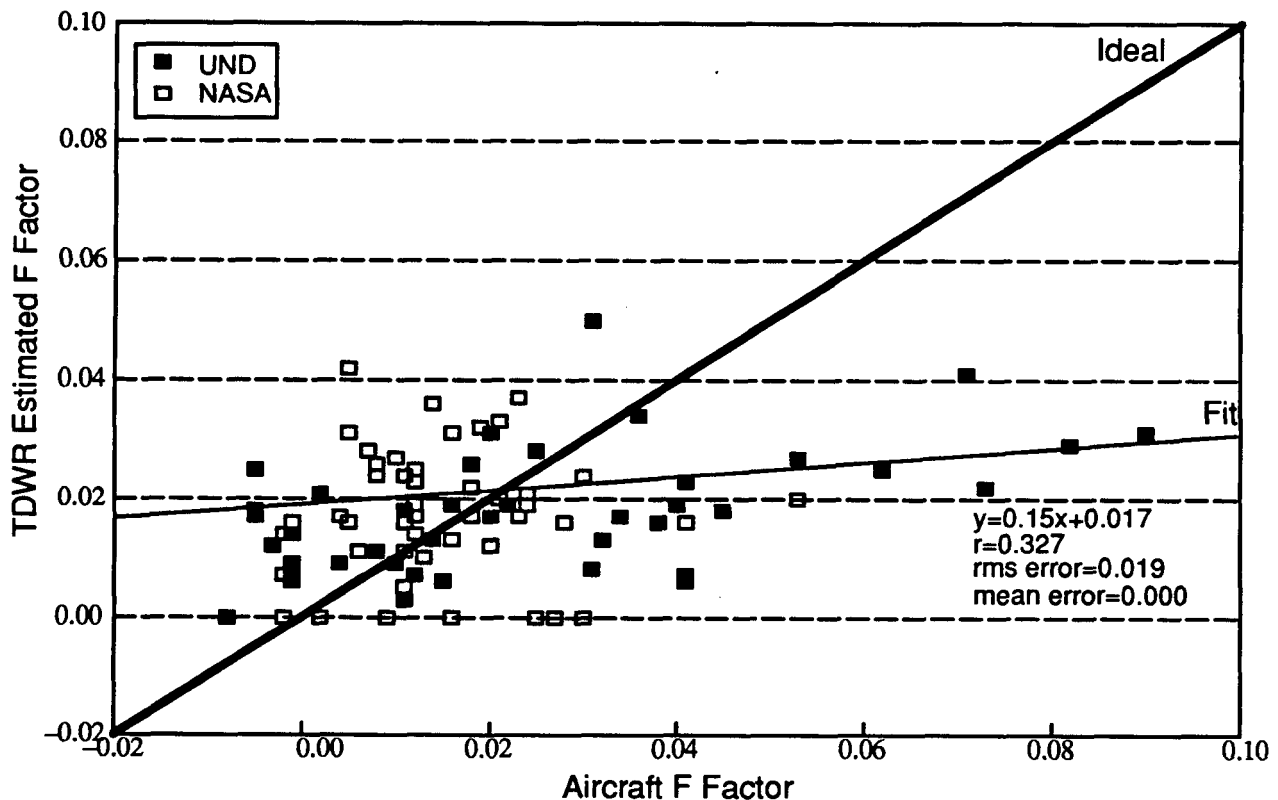


Figure 21. TDWR alarm vs. aircraft vertical F factor at F total peak time.

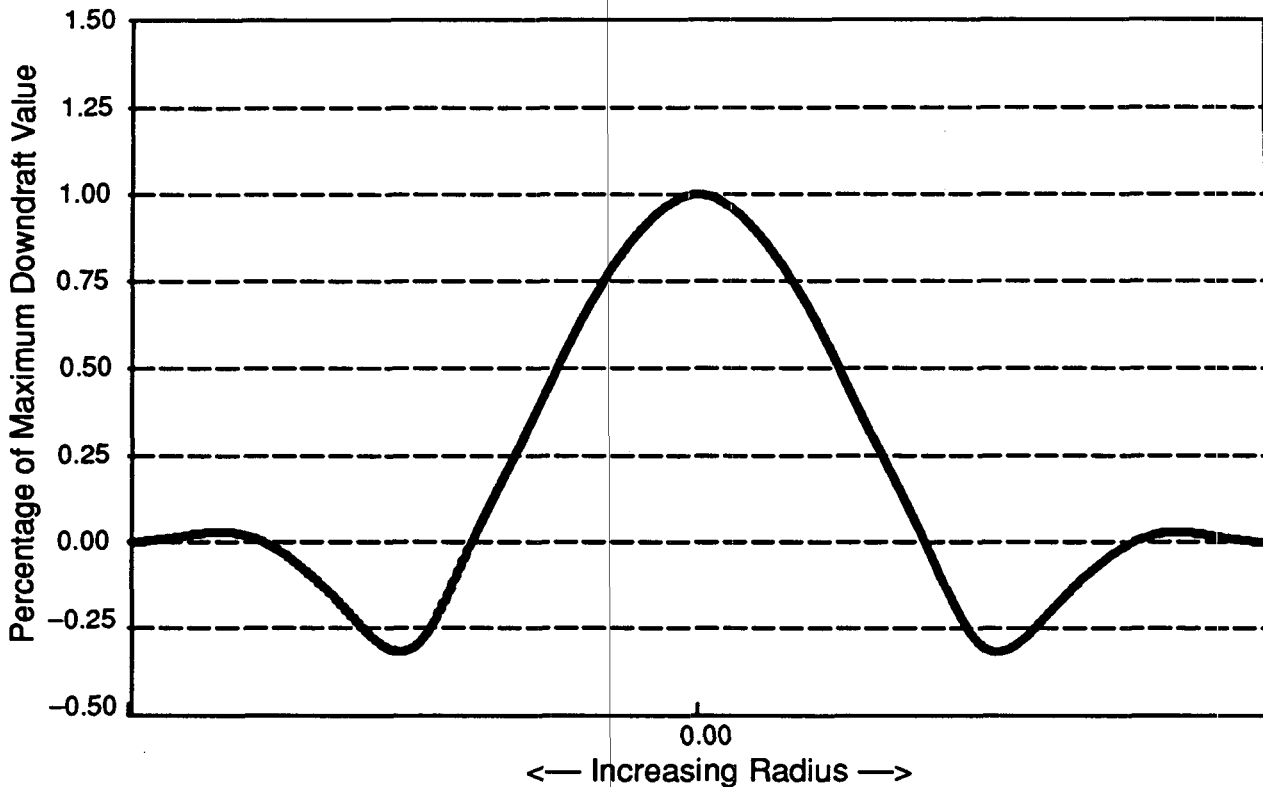


Figure 22. Downdraft profile across radius of microburst event in Vicroy Model.

microburst. In these cases, it is inevitable that equation (6.2) will estimate a vertical F factor that is not representative of the regions of the microburst that the aircraft penetrated.

Figure 23 shows the shear map estimated vertical component versus the *in situ* F factor. It is obvious that a better estimation of the vertical component needs to be developed. Most distressing are the numerous events in which the downdraft has been significantly *underestimated*. This may be the biggest problem of the shear map technique: it has no way to predict the presence of a downdraft without the presence of a horizontal shear component. If the outflow is tilted from vertical (perhaps due to ambient wind conditions) or if the outflow had interference at a given point (perhaps from interactions with a nearby microburst), the shear map will not identify the magnitude or location of the downdraft correctly at any point in the storm.

#### 6.6. F FACTOR ESTIMATES FROM ITWS MICROBURST ALGORITHM

Figure 24 is a comparison of the horizontal F factor after altitude compensation as estimated from ITWS with the *in situ* horizontal F factor. A comparison of Figure 13 and Figure 24 illustrates the improved horizontal F factor representation the ITWS detection algorithm gives over the TDWR microburst detection algorithm. More impressively, the ITWS performance in Figure 24 is comparable to the results from the TDWR shear map in Figure 17. Figure 25 demonstrates that the ITWS microburst algorithm estimates the vertical F factor as accurately as the TDWR shear map.

Another goal of the ITWS microburst algorithm is to more accurately characterize the size of the hazard presented to an aircraft from wind shear. To do this, the along-track trajectory total

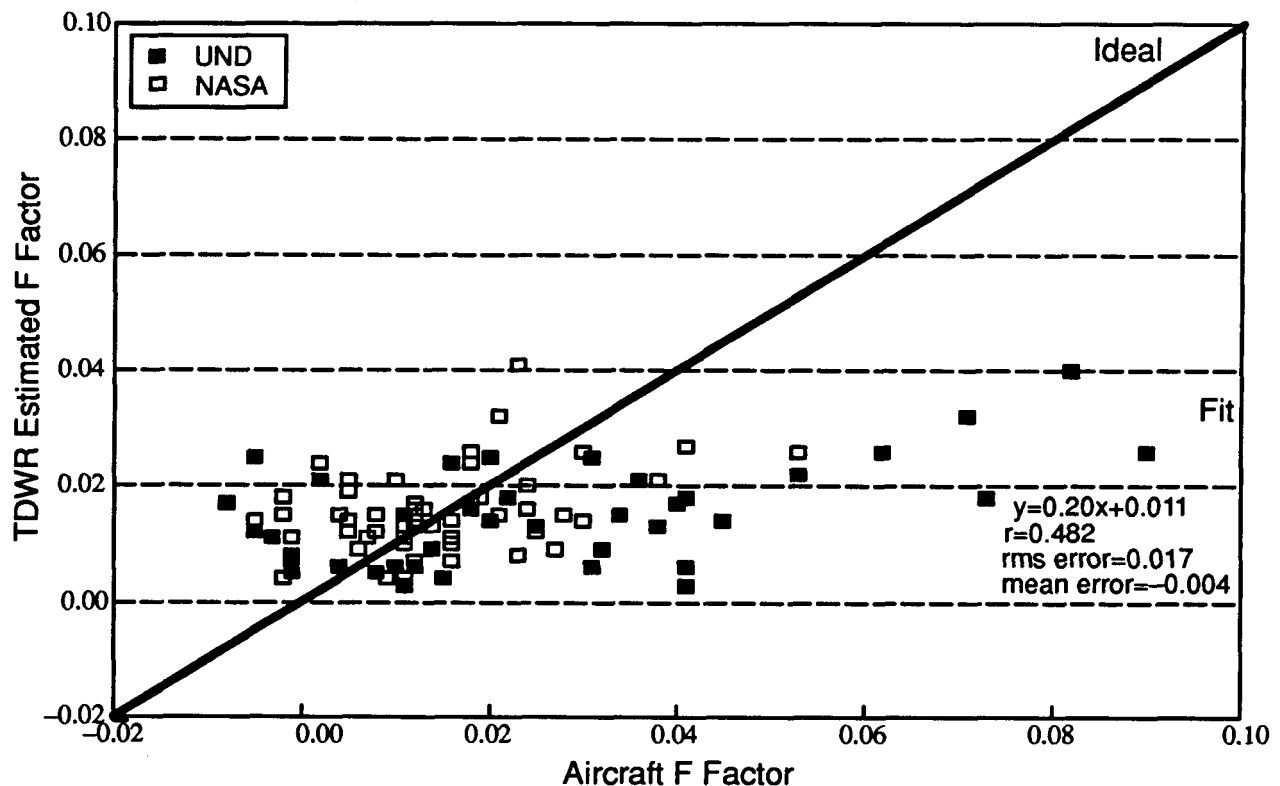


Figure 23. TDWR shear map vs. aircraft vertical F factor at F total peak time.

F factor can be compared to the estimated F factor at every second. Figure 26 is a comparison of the F factor for the TDWR microburst algorithm, the ITWS microburst algorithm, and the *in situ* F factor for a NASA penetration of a 6/15/91 event at 19:52 UT in Orlando, Florida. The dashed thick line is F factor estimated from the TDWR algorithm, and the solid thick line is the F factor estimated from ITWS. Figure 26 clearly shows that the ITWS algorithm can calculate an F factor which is more representative of what the aircraft experiences. The corresponding TDWR and ITWS shapes for this event are shown in Figure 27 and Figure 28 superimposed on the TDWR shear map from that time sample. The white line in Figure 27 and Figure 28 indicates the track of the NASA aircraft. The ITWS shape in Figure 23 is more indicative of a single microburst event, is smaller, and thus should reduce overwarning, and specifically highlights the region of strong shear with an additional shape.

Of the events in Figure 24 with no ITWS detection (ITWS shear output was zero), there are three possible explanations. First, the F factor experienced by the aircraft was not a hazard, thus the ITWS was not required to issue a detection. Events in which the aircraft experienced an F factor less than 0.105 are not considered a hazard. Second, some events penetrated by the aircraft were in their development stages. Since the TDWR is only capable of measuring horizontal outflow once per minute, any event in its development stage may go undetected. A solution to this problem is to incorporate the ITWS microburst detection product, which provides information about the projected location and intensity of developing microbursts. Finally, the aircraft flew along a track which fell just outside an ITWS icon. The ITWS detection algorithm is being tuned with this and other information to more accurately account for the extents of the hazard.

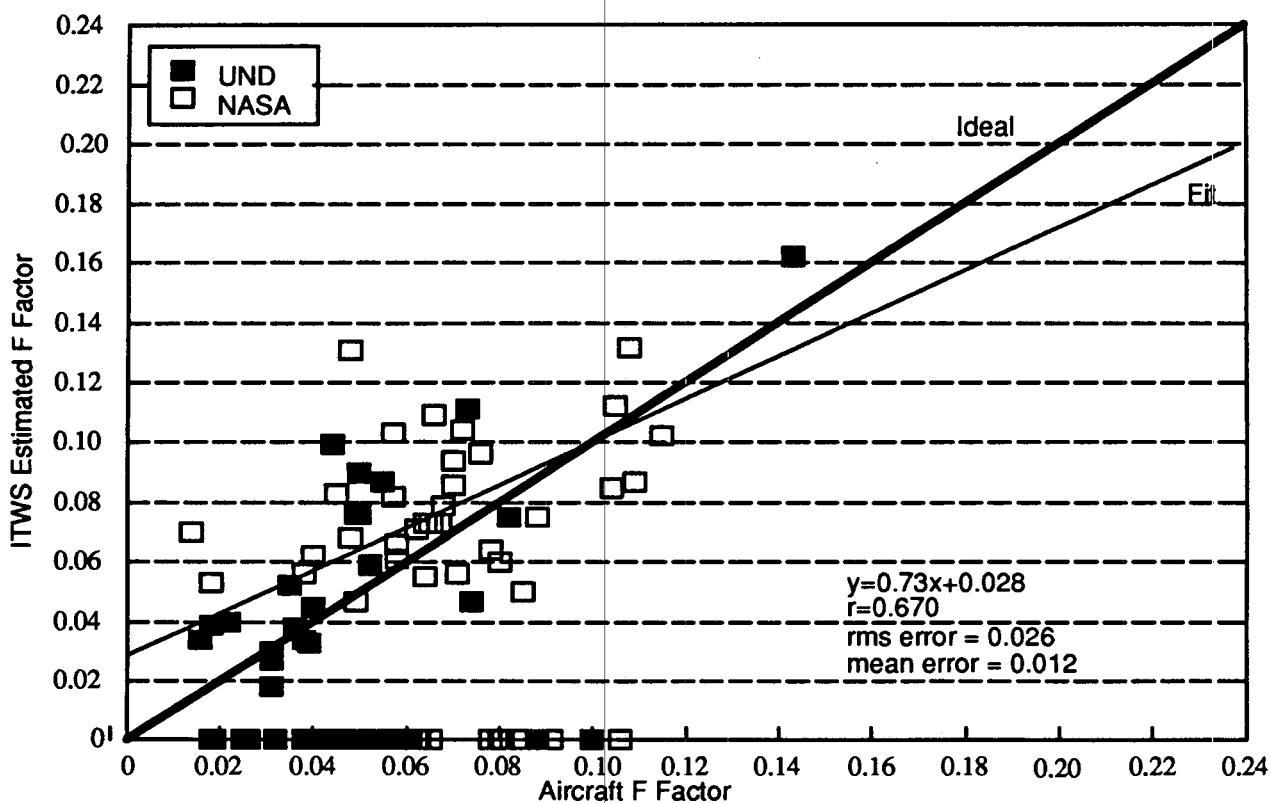


Figure 24. ITWS shape vs. aircraft horizontal F factor at F total peak time.

Several improvements are expected to be made in both the F factor estimation algorithm and the ITWS detection algorithm. First, a function will be added which corrects vertical F factor estimates for the distance from the center of the microburst. This is particularly crucial for the ITWS algorithm, which has the philosophy of alerting with one icon per event. Secondly, ongoing data analysis efforts are underway to determine the accuracy and overall performance of the ITWS microburst detections. As more results become available, changes will be made in the methods to further refine the ITWS microburst algorithm. Also, future work on the ITWS algorithm is planned to incorporate data from the Low Level Wind Shear Alert System (LLWAS). This should improve ability to detect asymmetric microbursts by providing data which is perpendicular to the radar beam (Hallowell, 1993), and ensure a consistent wind shear alert from systems within the terminal area.

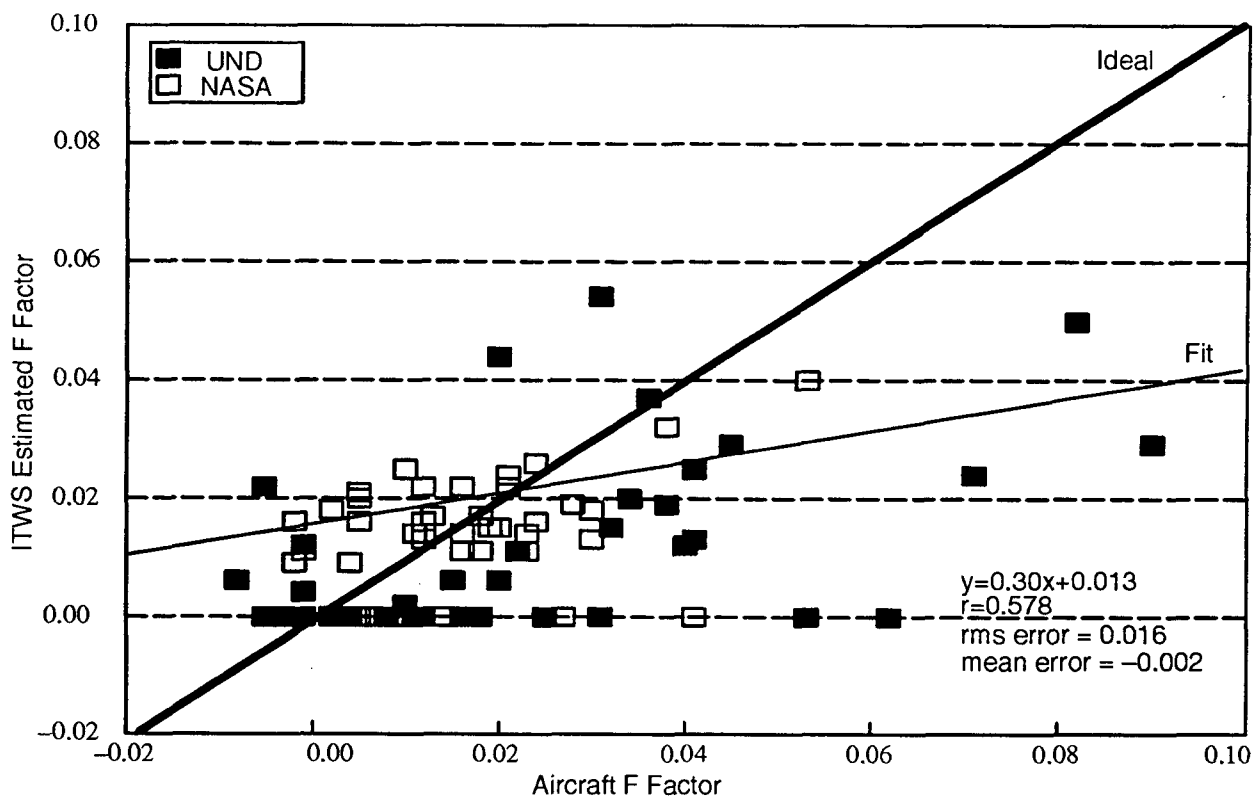


Figure 25. ITWS shape vs. aircraft vertical F factor at F total peak time.

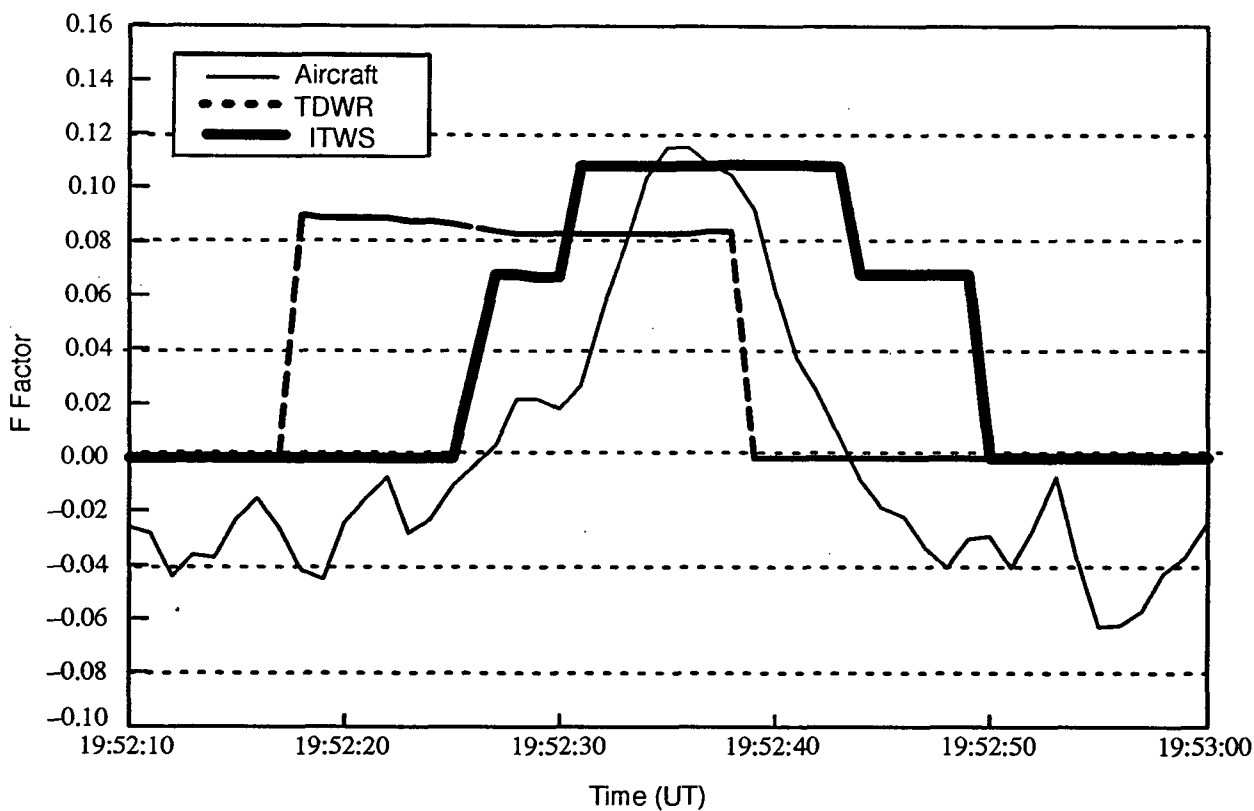
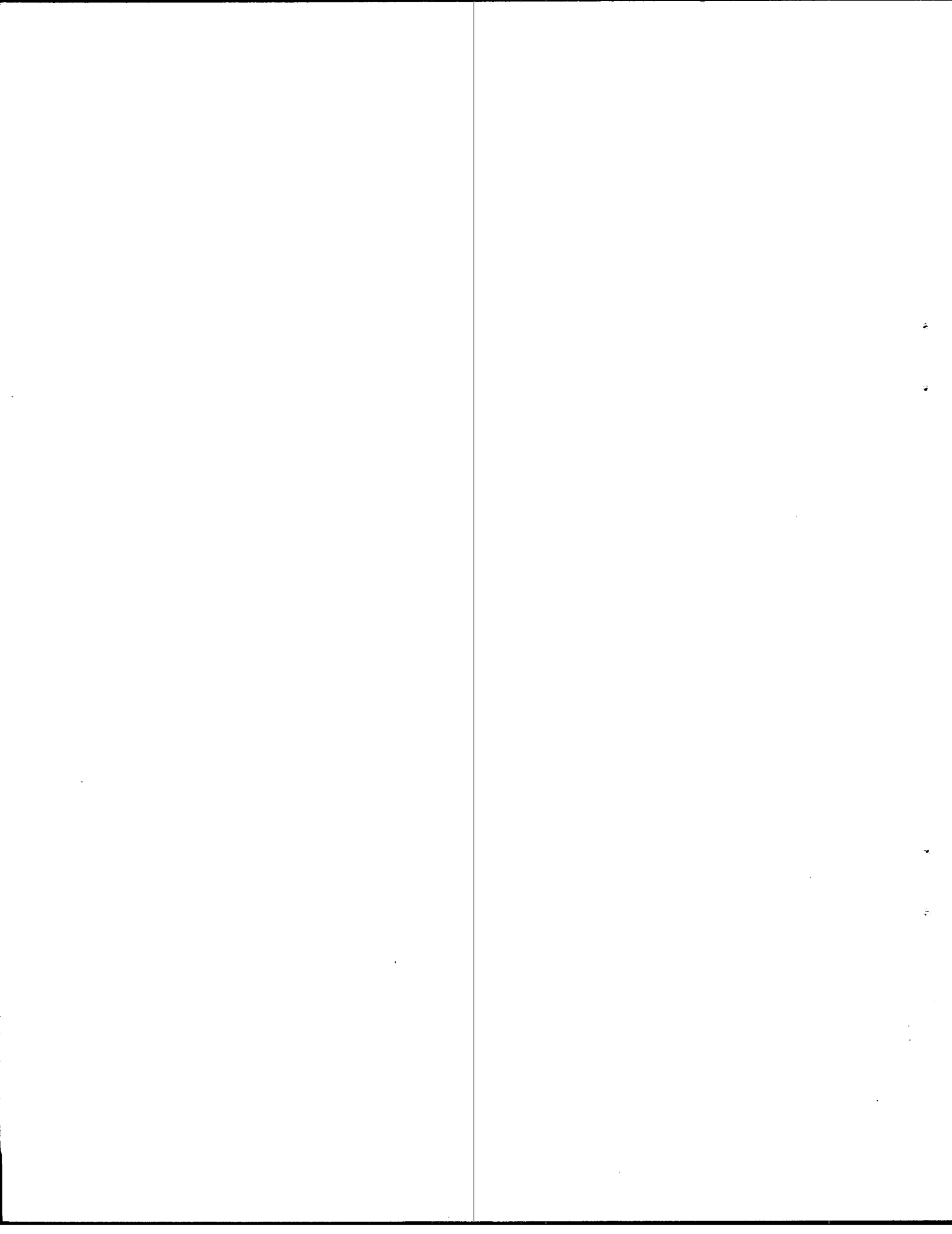


Figure 26. F factor estimated from TDWR and ITWS for NASA case on 6/15/91 in Orlando.



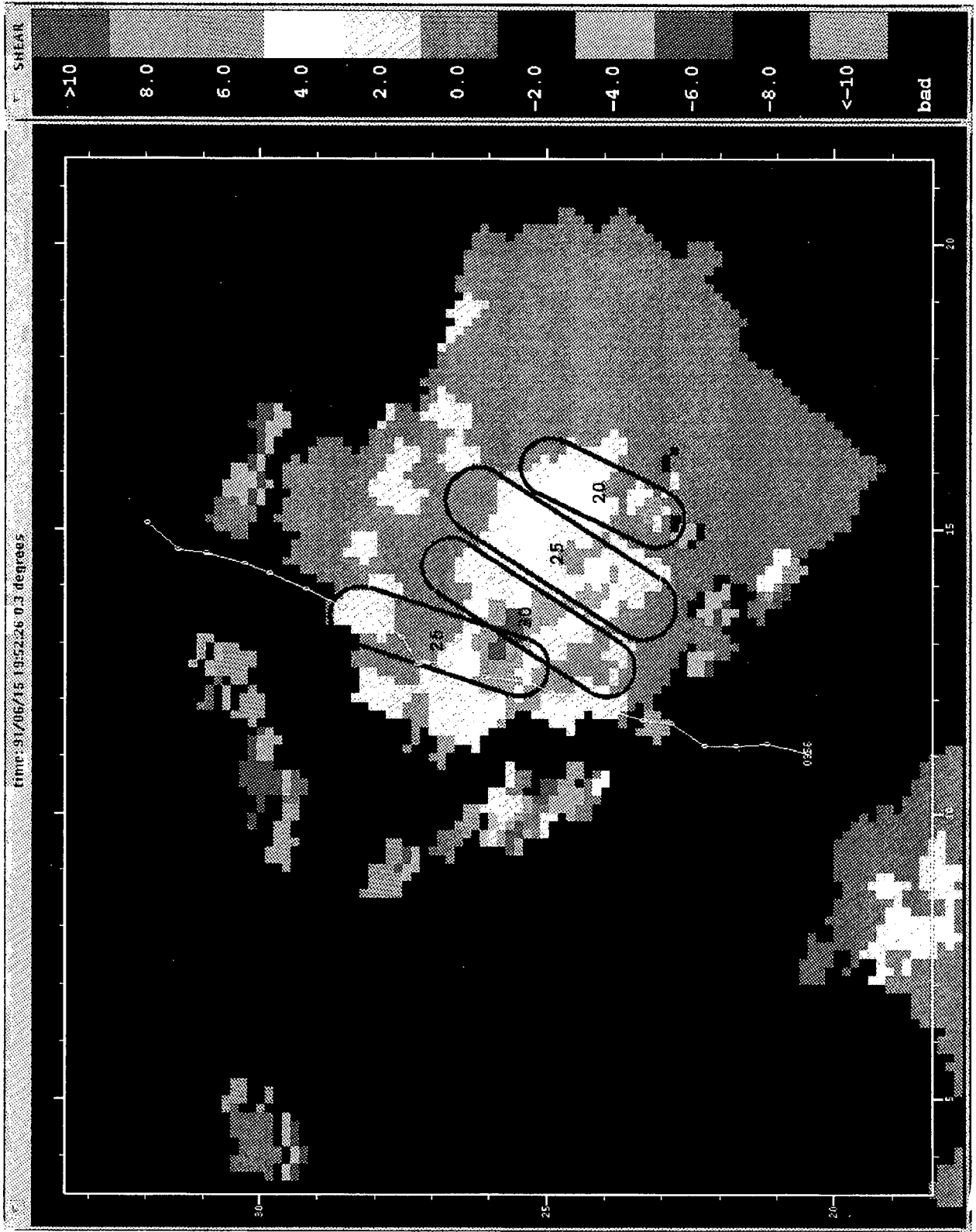
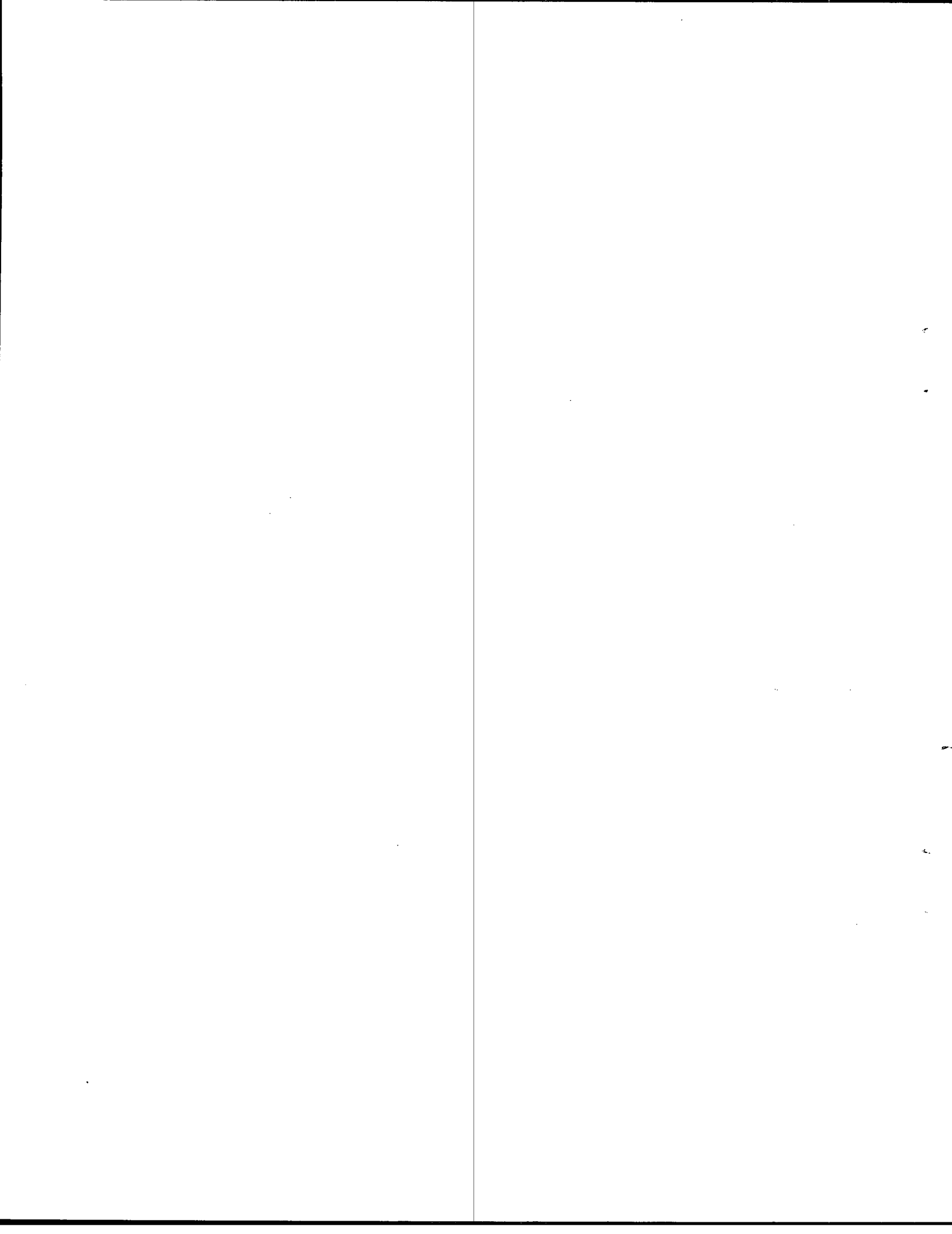


Figure 27. Shear map for NASA case on 6/15/91 in Orlando overlaid with TDWR shapes.



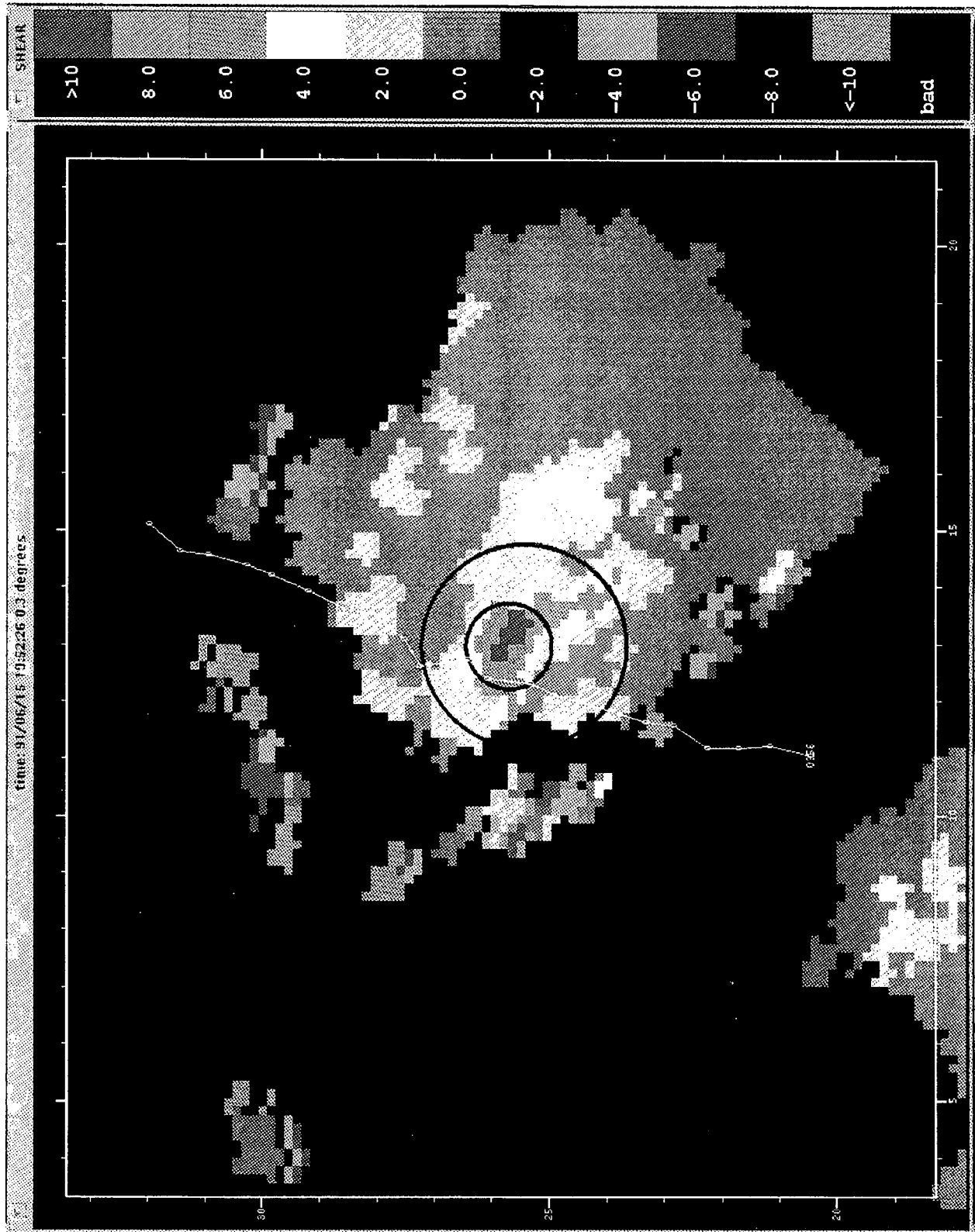
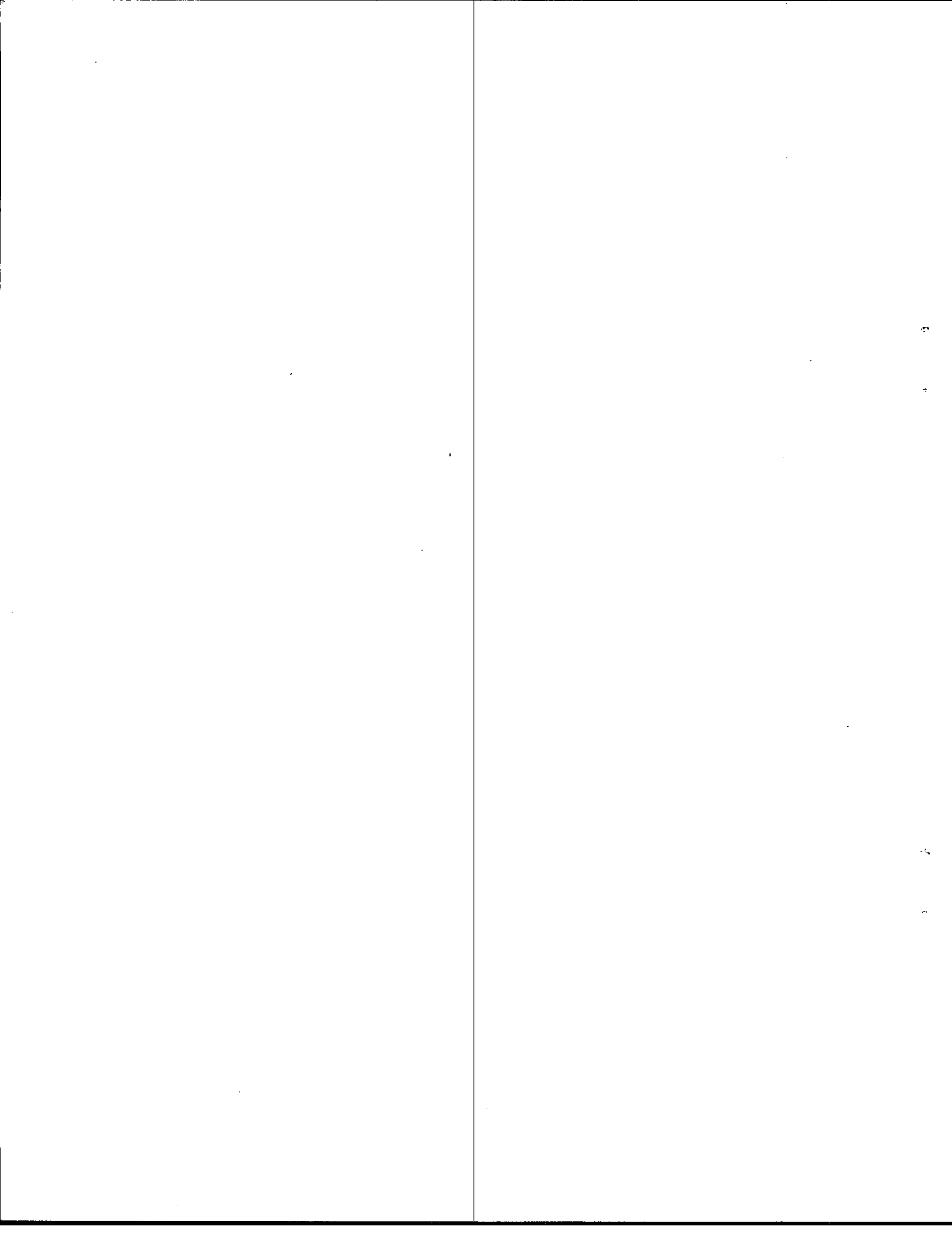


Figure 28. Shear map for NASA case on 615191 in Orlando overlaid with ITWS shapes.



## 7. IMPROVED RUNWAY ALERTING STRATEGY

The final task to be addressed by the CWI program is the development of a new runway alerting strategy based upon what has been learned in the program. Developing a new ground-based runway alerting strategy would be advantageous for three reasons. First, the airborne forward looking wind shear detection systems have been developed using different terminology and methods for characterizing the severity of a microburst from ground-based systems. The new runway alerting strategy would aim to eliminate this confusion. Second, it is in the best interest of the controller to know what actions a pilot may take based upon the pilot's wind shear information. Since the airborne systems have two levels of alert, it would be useful for the controller to be aware of what type of an alert the pilot is likely to see on the airborne radar display. The new runway alerting strategy will attempt to provide the controller with warnings similar to those seen by the pilot. Finally, the ground-based systems should provide the pilots lacking forward looking wind shear detection systems with the most accurate wind shear information available.

The improved runway alerting strategy should be based upon the ITWS microburst detections. Some work has suggested that the F factor could be computed directly from a shear map. However, due to the Doppler radar's single viewing angle, shear cannot be computed for all flight paths. An airborne Doppler radar does not have this problem because it is traveling in the same direction as the radar beam. This is especially true in the case of an F factor calculation because the F factor is not only dependent on altitude and aircraft speed, but is also dependent upon direction. Therefore, any estimation of F factor from a ground-based system should be based on a symbolic microburst detection by an automated microburst detection algorithm and not on the shear map.

There are several advantages of using the ITWS microburst detection algorithm to generate runway alerts. First, the new algorithm uses the shear map to detect microburst signatures. Second, a series of segmentation and grouping routines in the algorithm attempts to define one microburst shape for each microburst. Third, the ITWS algorithm can incorporate information about features aloft and other ITWS products, such as microburst prediction to properly estimate the vertical term of the F factor equation. Finally, a microburst model can be fitted to the microburst detections to accurately predict the F factor at all points within a microburst, eliminating the need for shear integration.

The new runway alerting strategy proposed under the CWI program would produce the following RDT message:

**18LA WSL SEV. 2MF 120 08**

A controller would read the message to the pilot on final approach as follows, "Eighteen left approach wind shear with loss, severe, two miles final." This indicates to the pilot that the approach corridor to runway 18L is impacted by a wind shear event with a loss of a severe intensity, with the first encounter beginning at two miles final.

The message would be composed of two possible wind shear categories: a wind shear with loss and a wind shear with gain. Furthermore, each wind shear category would have three pos-

sible severity levels: weak, moderate, and severe. Since the airborne systems are broken into three categories, the ground-based systems levels should correspond in some sense to the three airborne levels. Therefore, a pilot seeing a wind shear with loss classified as weak would not be likely to take any evasive actions. However, the pilot should be aware of the presence of wind shear. Likewise, a moderate wind shear event would advise the controller and pilot that the wind shear on the flight path may not set off an airborne alert, but is significant enough to warrant caution. Finally, a wind shear with loss of severe intensity would advise the pilot and controller that the on-board wind shear system would most likely issue an alert requiring an executive action or a missed approach. It is proposed that these three levels are based upon the F factor thresholds defined in the airborne systems. The thresholds should be: 0.04 to less than 0.85 is a weak wind shear, 0.85 to 0.13 is moderate, and greater than 0.13 is severe. This new runway alerting strategy would eliminate the reference to microburst from the ribbon display.

The proposed new runway alerting strategy is a major change from the alerting strategy that is currently being implemented in the TDWRs being deployed throughout the country. Such a change would require retraining on the use of the system and some reclarification of what constitutes a hazard. However, such changes are warranted by the deployment of the airborne systems, and the knowledge gained through the CWI program.

## 8. SUMMARY

This project report summarizes the CWI program at M.I.T. Lincoln Laboratory, funded through NASA Langley Research Center by the joint NASA/FAA Integrated Airborne Wind Shear program. The Fiscal Year 1993 marked the fourth year of a projected four-year program. The goals of the CWI program were accomplished during the four-year time frame.

Support of microburst penetrations by the research aircraft were accomplished in the wet microburst environment of Orlando, Florida. The testbed TDWR operated by Lincoln Laboratory provides real-time microburst information to the aircraft and the necessary meteorological and wind shear data to the research teams for their purposes. The CWI program also was successful in demonstrating the feasibility of a cockpit display of the TDWR wind shear products. During the NASA microburst penetrations, Lincoln and NASA were able to integrate ground-based and airborne wind shear information to provide crew-centered hazard warning.

Under the NASA program, Lincoln post processed the aircraft data and the TDWR data for each of the microburst penetrations and compared a hazard index, called the F factor. Post-flight processing was performed on data from four of the five test aircraft and analysis was performed to compare the aircraft data with three methods of equating the F factor from the TDWR radar. The first technique evaluated the use of the current TDWR microburst algorithm output to compute the hazard index. It was shown that calculating the F factor in this manner produced a very conservative estimate of the hazard posed by a microburst. The *in situ* F factor rarely exceeded the TDWR F factor estimate in magnitude, but the correlation between the two was poor. The second method calculated the F factor directly from radar radial velocity measurements which were differentiated to create a radial shear map. The overall results of this technique showed an improved correlation with the *in situ* measurements. However, decomposing the F factor estimate into its constituent horizontal (shear) and vertical (downdraft) components revealed the need for additional corrections to the ground-based estimate.

In particular, the horizontal component of the F factor was overestimated due to the dependence of outflow strength on altitude. The radar beam was usually scanning the strongest part of the outflow (~90 meters) while the plane penetrated the microburst at a higher altitude (~400 meters) where the outflow was weaker. To correct for this effect, the Oseguera & Bowles altitude profile for outflow strength vs. altitude was applied to the data. This correction brought the horizontal component of the F factor estimate into excellent agreement with the *in situ* data; however, the accuracy of the shear map estimates of the F factor vertical component remained poor.

The failure of the shear map based estimate to correctly infer the downdraft velocity was the limiting factor in its accuracy. The poor performance was primarily due to the simplistic assumption that the downdraft at any given point in a storm is directly proportional to the magnitude of the horizontal shear at that same point. This is an incorrect assumption, and a more sophisticated mechanism for estimating the downdraft velocity must be developed.

While the current TDWR microburst algorithm performs extremely well in detecting microburst hazards, some enhancements are needed to improve its ability to characterize the hazard in terms of F factor. A shear-based approach was developed which allows the horizontal F factor component to be estimated accurately. However, the vertical component remains poorly estimated due to an overly simplistic mass continuity assumption.

Although the CWI program has met its milestones and has been completed successfully, work continues on developing new F factor estimation techniques under the ITWS program. This work includes developing a shear-based microburst detection algorithm, developing better vertical F factor estimation techniques, and incorporating non-TDWR sensors to better detect asymmetric microbursts. The new microburst detection algorithm will attempt to eliminate the discrepancies between the current ground-based microburst detection systems and the forward-looking wind shear system being installed in the coming years.

The CWI program at Lincoln under the NASA/FAA Integrated Airborne Wind Shear program has had a major effect on the understanding of the microburst hazard. This new technology has led to the development of an improved ground-based microburst detection algorithm under the ITWS program. Future work on the ITWS microburst algorithm will depend heavily on the instrumented microburst penetrations conducted under the CWI program. No future work is expected in the CWI program.

## GLOSSARY

AGL	Above Ground Level
ASCII	American Standard Code for Information Interchange
ATOPS	Advanced Transport Operating System
CRT	Cathode Ray Tube
CWI	Cockpit Weather Information
dB	decibel
dBZ	decibel (referenced to reflectivity factor z)
DQE	Data Quality Edited
EAMED	Electronic Airborne Multipurpose Electronic Display
FAA	Federal Aviation Administration
GS	Ground Speed
GSD	Geographic Situation Display
Hz	Hertz
ILS	Instrument Landing System
INS	Instrument Navigation System
ITWS	Integrated Terminal Weather System
JAWS	Joint Airport Weather Studies
kW	Kilowatt
LAMBDA	Lincoln Advanced Microburst Detection Algorithm
LLWAS	Low Level Wind Shear Alert System
MCO	Orlando International Airport
MIT	Massachusetts Institute of Technology
NASA	National Aeronautics and Space Administration
NSSL	National Severe Storms Laboratory
PPI	Plan Position Indicator
PRF	Pulse Repetition Frequency

RDT	Ribbon Display Terminal
RNAV	Area Navigation
TAS	True Air Speed
TDWR	Terminal Doppler Weather Radar
TPS	Turbulence Prediction System
UND	University of North Dakota
VHF	Very High Frequency
VOR/DME	VHF Omni Range/Distance Measuring Equipment

## REFERENCES

- David M. Bernella, "Terminal Doppler Weather Radar Operational Test and Evaluation Orlando 1990," Lexington, MA, MIT Lincoln Laboratory, Project Report ATC-179, 9 April 1991.
- Roland L. Bowles, "Reducing Wind Shear Risk through Airborne Systems and Technology," *17th Congress on the Aeronautical Sciences*, Stockholm, Sweden, September 1990.
- C.L. Britt, and E. Bracalente, "NASA Airborne Radar Wind Shear Detection Hazard Algorithm and the Detection of Wet Microbursts in the Vicinity of Orlando Florida," *Airborne Wind Shear Detection and Warning Systems*, Fourth Combined Manufacturers' and Technologists' Conference, Williamsburg, Virginia, April 1992.
- Timothy J. Dasey, "A Shear Based Microburst Detection Algorithm for the Integrated Terminal Weather System (ITWS)," *26th International Conference on Radar Meteorology*, Norman, Oklahoma, May 24-28, 1993.
- Robert G. Hallowell, "Dual Doppler Measurements of Microburst Outflow Strength Asymmetry," *26th International Conference on Radar Meteorology*, Norman, Oklahoma, May 24-28, 1993.
- David A. Hinton, "Airborne Derivation of Microburst Alerts from Ground-Based Terminal Doppler Weather Radar Information," NASA TM-108990, August 1993.
- Michael S. Lewis, Kenneth R. Yenni, Harry A. Verstynen, and Lee H. Person, "Design and Conduct of a Windshear Detection Flight Experiment," AIAA 92-4092, presented at the AIAA 6th Biennial Flight Test Conference, Hilton Head, SC, August 24-26, 1992.
- Michael S. Lewis, P.A. Robinson, D.A. Hinton, and R.L. Bowles, "The Relationship of an Integral Wind Shear Hazard to Aircraft Performance Limitations," NASA TM-109080, February 1994.
- Rosa M. Oseguera, and Roland L. Bowles, "A Simple, Analytic 3-Dimensional Downburst Model Based on Boundary Layer Stagnation Flow," NASA TM-1000632, (July 1988).
- Rosa M. Oseguera, Roland L. Bowles, and Paul A. Robinson, "Airborne In Situ Computation of the Wind Shear Hazard," *AIAA 30th Aerospace Sciences Meeting and Exhibit*, Reno, NV, January 6-9, 1992.
- Timothy D. Sykes and Benjamin H. Stevens, "TDWR Velocity Dealiasing in Operation," *25th International Conference on Radar Meteorology*, American Meteorological Society, Paris, France, June 24-28, 1991.
- Dan D. Vicroy, "A Simple Analytical, Axisymmetric Microburst Model for Downdraft Estimation," NASA TM-104053, February 1991.

C. Wanke and R.J. Hansman, "Hazard Evaluation and Operational Cockpit Display of Hazardous Windshear Information," AIAA-90-0566, *AIAA 28th Aerospace Sciences Meeting and Exhibit*, Reno, NV, January 8-11, 1990.

C. Wanke and R.J. Hansman, "Experimental Evaluation of Candidate Graphical Microburst Alert Displays," AIAA-92-0292, *AIAA 30th Aerospace Sciences Meeting and Exhibit*, Reno, NV, January 6-9, 1992.